Pediatr Blood Cancer 2014;61:760–762

BRIEF REPORT
Two Cases of Neuroblastoma Comprising Two Distinct Clones

Fumito Yamazaki, MD,[1] Atsuko Nakazawa, MD, PhD,[2] Tomoo Osumi, MD,[1] Naoki Shimojima, MD, PhD,[3] Takeo Tanaka, MD, PhD,[4] Akira Nakagawara, MD, PhD,[5] and Hiroyuki Shimada, MD, PhD[1]*

We report two cases of high-risk metastatic neuroblastoma, comprising two biologically distinct components in the adrenal primary tumor, which showed clear differences not only histologically but also in *MYCN* amplification and *HA-RAS/TRKA* immunoreactivity (Case 1), anaplastic lymphoma kinase (ALK) immunoreactivity (Case 2). These two cases with multiple separated components were similar to cases classified as ganglioneuroblastoma, nodular subtype (GNBn), in terms of composite tumor. Comparable to the GNBn category, the prognosis of the patients described here may depend on the components with unfavorable histology according to International Neuroblastoma Pathology Classification. Further analyses of such composite neuroblastoma cases are important for assessing disease prognosis. Pediatr Blood Cancer 2014;61:760–762. © 2013 Wiley Periodicals, Inc.

Key words: ganglioneuroblastoma; international neuroblastoma pathology classification; neuroblastoma

INTRODUCTION

The International Neuroblastoma Pathology Classification (INPC) classifies peripheral neuroblastic tumors into four categories: neuroblastoma (Schwannian stroma-poor); ganglioneuroblastoma, intermixed (Schwannian stroma-rich); ganglioneuroma (Schwannian stroma-dominant); and ganglioneuroblastoma, nodular (GNBn) (composite: Schwannian stroma-rich/stroma-dominant, and stroma-poor) [1,2]. Among these four categories, only GNBn tumors are defined as composite tumors comprising histologically and biologically different clones. By definition, one of the tumor components in GNBn has features consistent with ganglioneuroblastoma, intermixed or ganglioneuroma, and the other has an appearance of neuroblastoma. Here, we report two cases of neuroblastoma comprising two histologically and biologically distinct clones, similar to the GNBn category in terms of having two or more different clones. However, this type of composite neuroblastoma could not be classified according to the current INPC system.

CASE PRESENTATION

Case 1. A 14-month-old male presented with intermittent fever for 2 months. Abdominal computed tomography (CT) revealed an approximately 4-cm left adrenal mass. After complete resection of the mass, he was diagnosed with neuroblastoma. Other sites of involvement included the lymph nodes and bone marrow: International Neuroblastoma Risk Group Classification (INRG) stage M. After surgery, the patient underwent induction/high-dose chemotherapy with autologous peripheral blood stem cell transplantation, radiation, and 13-cis-retinoic acid treatment. Complete remission has been maintained for 3 years since diagnosis.

Microscopically, the resected left adrenal gland tumor comprised two neuroblastoma nodular components separated by a fibrillary matrix (components A and B in Fig. 1a). Component A was classified as neuroblastoma, a poorly differentiated subtype with a high mitosis-karyorrhexis index (MKI); small round cells with almost bare nuclei surrounded by a few neuropils were observed (Fig. 1b). Component B was classified as neuroblastoma, poorly differentiated subtype with a low MKI; relatively large nuclear cells surrounded by abundant neuropils were observed. Component B was more differentiated compared with component A. Some cells in component B had abundant eosinophilic cytoplasm and were observed to be in the process of differentiating into ganglion cells (Fig. 1c). Schwannian cells were not identified by S-100 immunostaining in both component A and B. Lymph nodes around the left adrenal tumor and bone marrow contained metastatic tumor cells similar in appearance to component A cells. According to INPC, component A was classified into Unfavorable Histology Group and component B into Favorable Histology Group.

For each of the two components observed in the case, fluorescent in situ hybridization (FISH) using the LSI *MYCN* (2p24) SpectrumGreen/CEP 2 Spectrum Orange Probe (Vysis) was performed on formalin-fixed, paraffin-embedded material, and *HA-RAS/TRKA* expression patterns were immunohistochemically examined. Component A exhibited *MYCN* amplification and low *HA-RAS/TRKA* expression, whereas component B demonstrated *MYCN* non-amplification and high *HA-RAS/TRKA* expression. In contrast, array-based comparative genomic hybridization profiles of two components demonstrated similar patterns for chromosomal events as a prognostic marker, including deletions of chromosomes 1p and 11q and gain of chromosome 17q. *MYCN* amplification was presented only in component A, which was the same as shown in FISH analysis. Both components were classified within the genetic group of partial chromosomal gains and/or losses that indicate poor disease prognosis [3].

Case 2. A 21-month-old male presented with right hip pain and gradual bulging of his eyes for several days. Abdominal CT showed an approximately 8-cm right adrenal mass. He was diagnosed with

[1]Department of Pediatrics, Keio University School of Medicine, Tokyo, Japan; [2]Department of Pathology, National Medical Center for Child Health and Development, Tokyo, Japan; [3]Department of Pediatric Surgery, Keio University, School of Medicine, Tokyo, Japan; [4]National Hospital Organization Hiroshimanishi Medical Center, Hiroshima, Japan; [5]Department Division of Biochemistry, Chiba Cancer Center Research Institute, Chiba, Japan

Conflict of interest: Nothing to declare.

*Correspondence to: Hiroyuki Shimada, Department of Pediatrics, Keio University School of Medicine, 35 Shinanomachi, Shinjuku-ku, Tokyo 160-8582, Japan. E-mail: hshimada@a5.keio.jp

Received 4 July 2013; Accepted 22 August 2013

DOI 10.1002/pbc.24779
Published online 20 September 2013 in Wiley Online Library (wileyonlinelibrary.com).

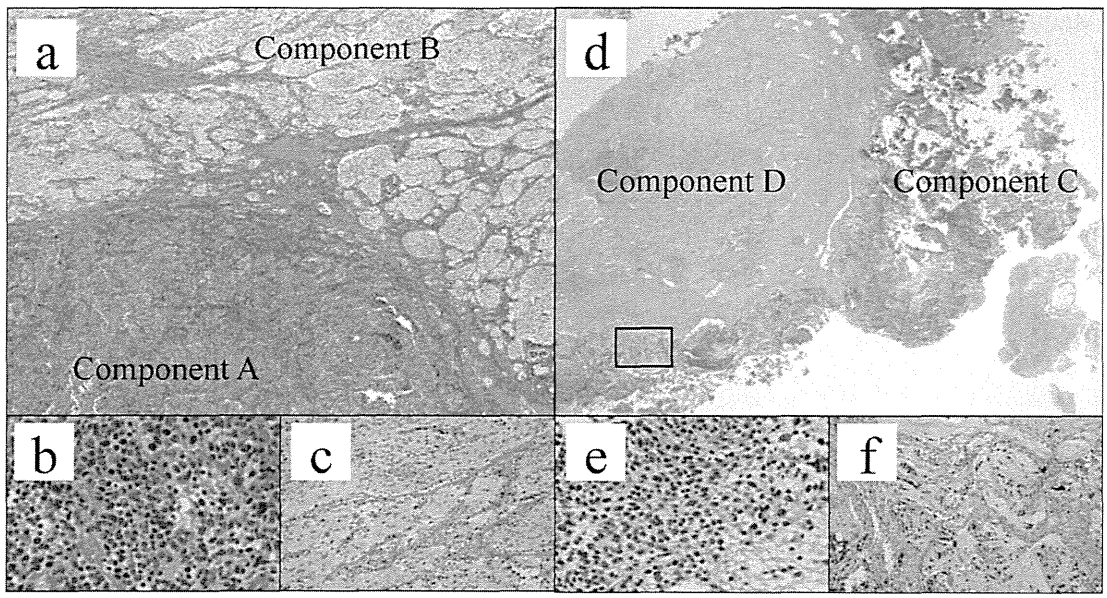

Fig. 1. **a**: The resected tumor in the left adrenal gland comprised two distinct components: component A (lower) and component B (upper). Case 1, H&E, 40×. **b**: Component A: neuroblastoma, a poorly differentiated subtype with a high mitosis-karyorrhexis index (MKI). H&E, 400×. **c**: Component B: neuroblastoma, a poorly differentiated subtype with a low MKI, more differentiated compared with component A.H&E, 400×. **d**: The tissue obtained at biopsy in the right adrenal gland comprised two distinct components: component C (right) and component D (left). Most Component D consisted of fibrous tissue with small foci of neuroblasts. A portion of Component D (square, Figure f) was classified as neuroblastoma, a differentiating subtype. Case 2, H&E, 40×. **e**: Component C: neuroblastoma, a poorly differentiated subtype with a high MKI. H&E, 400×. **f**: Component D: neuroblastoma, a differentiating subtype. H&E, 400×.

neuroblastoma following biopsy of the mass. Other sites of involvement included the lymph nodes, multiple bones, and bone marrow (INRG stage M). Because of the poor response to multidrug chemotherapy, a tandem transplantation was planned after abdominal tumor resection. Unfortunately, the patient died from sudden respiratory failure before the second transplantation.

Microscopically, the tissue obtained by biopsying the right adrenal gland before treatment comprised two neuroblastoma nodular components separated by a fibrillary matrix (components C and D in Fig. 1d). Component C was classified as neuroblastoma, a poorly differentiated subtype with a high MKI (Fig. 1e). Most of component D consisted of fibrous tissue with small foci of neuroblasts. A portion of component D was classified as neuroblastoma, a differentiating subtype. MKI could not be assessed because the number of neuroblastic cells was insufficient (<5,000 cells; Fig. 1f). Schwannian cells were not identified by S-100 immunostaining in both component C and D. Lymph nodes around the right adrenal tumor and bone marrow contained metastatic tumor cells similar in appearance to the cells of component C. According to INPC, component C was classified into Unfavorable Histology Group and component D into Favorable Histology Group. Both components exhibited *MYCN* non-amplification and high *HA-RAS/TRKA* expression. However, different patterns were observed in ALK expression analysis; components C and D showed high and low ALK immunoreactivity, respectively.

DISCUSSION

We present two cases of neuroblastoma comprising two histologically and biologically distinct neuroblastoma components. A similar case was previously reported by Sano et al. [4]; one component showed neuroblastoma, poorly differentiated subtype with a high MKI and *MYCN* amplification, whereas the other showed neuroblastoma, poorly differentiated subtype with a low MKI and *MYCN* non-amplification. INPC distinguished the two components into Unfavorable and Favorable Histology Groups. In addition to clear histological differences between the two components in Sano's case and our two cases, the components differed in *MYCN* amplification in Sano's case, *MYCN* amplification and *HA-RAS/TRKA* immunoreactivity in our Case 1, and ALK immunoreactivity in our Case 2. Similar to *MYCN* amplification and *Ha-ras/trkA* gene expression [5], ALK immunoreactivity is a significant predictor of disease prognosis [6,7]. These three cases indicate that the combination of two separate neuroblastoma components that histologically, immunohistochemically, and biologically vary depending on a case-by-case basis.

Our two cases were similar to tumors classified as GNBn in that they also showed multiple separated components (clones). Based on the similarity with GNBn, we propose describing the composite neuroblastomas reported here as neuroblastoma, nodular (NBn), as previously proposed by Sano et al. [4]. Nonaggressive components (ganglioneuroblastoma, intermixed or ganglioneuroma) of GNBn are classified as Favorable Histology in INPC and are considered to have differentiated from neuroblastoma based on the age-linked maturational sequence. If we can observe a GNBn tumor at an earlier age, the nonaggressive components may have the appearance of neuroblastoma with Favorable Histology in the first or second step of the age-linked maturational sequence, that is, poorly differentiated or differentiating neuroblastoma. This subtype is considered to correspond to NBn (Fig. 2).

Patients with GNBn can be divided into two prognostic subsets by applying the same age-linked morphological criteria used in

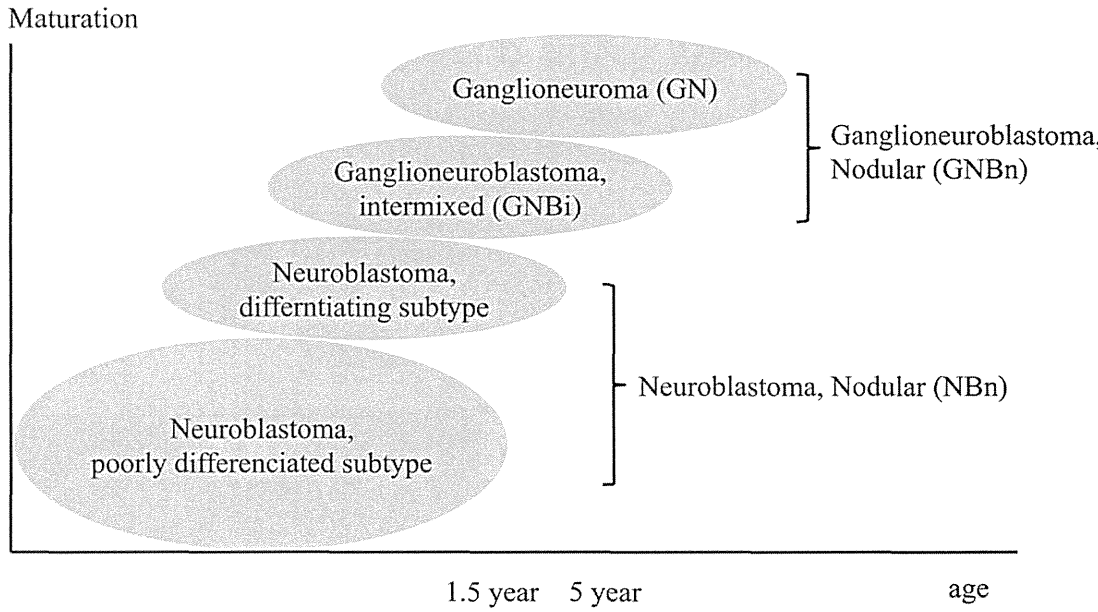

Fig. 2. The nonaggressive components classified as Favorable Histology of composite neuroblastic tumors (ganglioneuroblastoma, nodular (GNBn) and Neuroblastoma, nodular (NBn)) are considered to differentiate from poorly differentiated (<1.5 years of age at diagnosis) to differentiating (<5 years of age) neuroblastomas to ganglioneuroblastoma, intermixed and to ganglioneuroma based on the age-linked maturational sequence. Ganglioneuroblastoma, intermixed or ganglioneuroma are the feature of nonaggressive components in GNBn, while poorly differentiated or differentiating neuroblastoma are the feature of those in NBn.

neuroblastoma category to their neuroblastoma components: favorable and unfavorable subsets. The difference in estimated survival between these two subsets of GNBn patients is statistically significant [8]. Therefore, the INPC system was modified to account for this difference [9]. If the same principle is applied, NBn patient prognosis should depend on the components with unfavorable histology. Although histological and molecular intratumoral heterogeneity was previously reported in neuroblastoma with transition from one component to the other [10,11], two different tumor components (Favorable and Unfavorable Histology Groups) were clearly distinguishable and separately identifiable in NBn, including our cases. *MYCN* analysis by FISH with paraffin sections and immunohistochemical analysis for ALK were critical for precisely identifying the two histologically and biologically different neuroblastoma components. Further analyses of NBn patients are needed to assess disease prognosis by obtaining a sufficient amount of tumor tissues for precise phenotypic and genotypic evaluations.

REFERENCES

1. Shimada H, Ambros IM, Dehner LP, et al. The international neuroblastoma pathology classification (the Shimada system). Cancer 1999;86:364–372.
2. Shimada H, Ambros IM, Dehner LP, et al. Terminology and morphologic criteria of neuroblastic tumors: Recommendations by the International Neuroblastoma Pathology Committee. Cancer 1999;86:349–363.
3. Ohira M, Nakagawara A. Global genomic and RNA profiles for novel risk stratification of neuroblastoma. Cancer Sci 2010;101:2295–2301.
4. Sano H, Gonzalez-Gomez I, Wu SQ, et al. A case of composite neuroblastoma composed of histologically and biologically distinct clones. Pediatr Dev Pathol 2007;10:229–232.
5. Kyo Y, Tanaka T, Hayashi K, et al. Identification of therapy-sensitive and therapy-resistant neuroblastoma subtypes in stages III, IVs and IV. Cancer Lett 2011;1:27–33.
6. Duijkers FA, Gaal J, Meijerink JP, et al. High anaplastic lymphoma kinase immunohistochemical staining in neuroblastoma and ganglioneuroblastoma is an independent predictor of poor outcome. Am J Pathol 2012;180:1223–1231.
7. Passoni L, Longo L, Collini P, et al. Mutation-independent anaplastic lymphoma kinase overexpression in poor prognosis neuroblastoma patients. Cancer Res 2009;69:7338–7346.
8. Umehara S, Nakagawa A, Matthay KK, et al. Histopathology defines prognostic subsets of ganglioneuroblastoma, nodular. Cancer 2000;89:1150–1161.
9. Peuchmaur M, d'Amore ES, Joshi VV, et al. Revision of the international neuroblastoma pathology classification: Confirmation of favorable and unfavorable prognostic subsets in ganglioneuroblastoma, nodular. Cancer 2003;98:2274–2281.
10. Ambros PF, Ambros IM, Kerbl R, et al. Intratumoral heterogeneity of 1p deletions and MYCN amplification in neuroblastomas. Med Pediatr Oncol 2001;36:1–4.
11. Thorner PS, Ho M, Chilton-MacNeill S, et al. Use of chromogenic in situ hybridization to identify MYCN gene copy number in neuroblastoma using routine tissue sections. Am J Surg Pathol 2006;30:635–642.

Cancer Letters xxx (2014) xxx–xxx

Contents lists available at ScienceDirect

Cancer Letters

journal homepage: www.elsevier.com/locate/canlet

RASSF1A methylation may have two biological roles in neuroblastoma tumorigenesis depending on the ploidy status and age of patients ☆

Masayuki Haruta [a], Takehiko Kamijo [b], Akira Nakagawara [b], Yasuhiko Kaneko [a,*]

[a] *Research Institute for Clinical Oncology, Saitama Cancer Center, Ina, Saitama, Japan*
[b] *Research Institute, Chiba Cancer Center, Chiba, Japan*

ARTICLE INFO

Article history:
Received 3 September 2013
Received in revised form 19 March 2014
Accepted 19 March 2014
Available online xxxx

Keywords:
Neuroblastoma
Mass-screening
RASSF1A methylation
Triploid
Diploid

ABSTRACT

RASSF1A methylation was frequent in neuroblastomas found in infants by mass-screening or infants and children diagnosed clinically, whereas *CASP8* and *DCR2* methylation was only frequent in tumors in children. When classified according to the ploidy status, *RASSF1A* and *PCDHB* methylation was only associated with *MYCN* amplification and poor outcomes in infants with a clinically diagnosed diploid, not triploid tumor. *RASSF1A* and *PCDHB* methylation was associated with poor outcomes in children with triploid and diploid tumors, respectively, and with *MYCN* amplification in children with diploid tumor. *RASSF1A* methylation may have two biological roles based on the ploidy status and patient's age.

1. Introduction

Neuroblastoma is the most common solid tumor in children, and accounts for 8–10% of childhood cancers and 15% of childhood cancer deaths [1]. While localized neuroblastomas in infants regress spontaneously or mature, disseminated tumors in children resist intensive multimodal treatment [2,3]. A mass-screening program has been conducted on infants in Japan and other countries, based on the assumption that the early detection of tumors in infants could improve overall outcomes [4–6]. Because it is clear that damage has been caused by excessive treatment of some neuroblastomas that would have regressed spontaneously, and the effectiveness of the program has been questioned [5–7], this program was discontinued in Japan.

RASSF1A functions as a tumor suppressor gene that plays an important role in cell cycle arrest, apoptosis, genomic stability, microtubule stabilization, and cell motility [8–10]. The mRNA expression levels of *RASSF1A* are controlled by DNA methylation in the promoter region, and it is a representative gene that shows hypermethylation in various primary tumors [8,11–24]. Caspase 8 encoded by *CASP8* is a family member of cysteine proteases that play essential roles in apoptosis, and silencing of *CASP8* by methylation has frequently been found in neuroblastomas, especially those with *MYCN* amplification [14–19,21,22,24–28]. DCR2 has been shown to prevent binding of TNF-related apoptosis-inducing ligand (TRAIL) to the death receptors, DR4 and DR5 as a decoy receptor, and exhibits antiapoptotic activity. The down-regulation of *DCR2* by promoter methylation was reported in various types of cancer including neuroblastoma [29,30]. In addition, the CpG island methylator phenotype (CIMP) was shown to have stronger prognostic power than methylation of individual genes in neuroblastomas; CIMP was detected by methylation analysis of the *PCDHB* CGIs [31].

Tumor cell ploidy is one of the biomarkers that predicts outcomes of patients with neuroblastoma. The majority of tumors found by mass-screening have been characterized by triploidy [32]. The International Neuroblastoma Risk Group (INRG) classification system used ploidy (DNA index) to classify tumors with distant metastasis and less than 18 months of age [33].

Many studies have examined the methylation status of tumor suppressor genes in neuroblastomas; however, none have clarified the association between methylation of the genes and the subtypes of tumors classified by age, method for tumor detection, or the ploidy status, although the disease is well-known for its biological heterogeneity [14–28]. We found that *RASSF1A*, *CASP8*, *DCR2*, and *PCDHB* family were significantly methylated, and associated with clinical and *MYCN* status. When tumors were classified according

☆ Grant sponsors: The Ministry of Health, Welfare and Labor of Japan (for Second-Term Comprehensive 10-Year Strategy for Cancer Control).

* Corresponding author at: Division of Cancer Diagnosis, Research Institute for Clinical Oncology, Saitama Cancer Center, Ina, Saitama, Japan. Tel.: +81 48 722 1111; fax: +81 48 723 5197.
E-mail address: kaneko@cancer-c.pref.saitama.jp (Y. Kaneko).

http://dx.doi.org/10.1016/j.canlet.2014.03.022
0304-3835/

to the ploidy status, *RASSF1A* and *DCR2* methylation was associated with poor outcomes in infants with a diploid, not triploid tumor, and in children with a triploid, not diploid tumor, suggesting age-dependent heterogeneity in triploid tumors.

2. Material and methods

2.1. Patients and samples

Tumors were obtained from 259 Japanese infants or children with neuroblastoma who underwent biopsy or surgery between January 1985 and December 1998. One-hundred and twenty-three patients were found by mass-screening to have neuroblastomas at 6 months of age (group A1) and 64 patients at 18 months of age or less (group A2), and 72 children over 18 months (group B) were diagnosed clinically.

2.2. Ploidy determined by interphase FISH and flow cytometry

Pathologists in each institution verified that each sample contained 70% or more tumor cells. To detect the copy number of chromosome 1s and the status of 1p, two-color FISH was performed using the two probes, D1Z1 and D1Z2, as described previously [34]. Disomy 1, trisomy 1, tetrasomy 1, or pentasomy 1 was determined based on the number of D1Z1 signals. The DNA index of tumor tissues was analyzed on the Becton–Dickinson FACScan flow cytometer by DNA cell-cycle analysis software-version C. Tumors were classified into 2 types (diploid, 2n and triploid, 3n) based on the numbers of chromosome 1 or the DNA index obtained by flow cytometry. Triploidy included triploidy and hyperdiploidy determined by flow cytometry, and tumors with a combination of cells with 3, 4, and 5 chromosomes 1 examined by FISH were classified as triploid (3n) tumors.

2.3. Sodium bisulfite modification and conventional methylation-specific PCR (MSP) analysis

Bisulfite treatment was performed as previously described [11,35]. The genes examined were *RASSF1A*, *CASP8*, *DCR2*, *HOXA9*, *RUNX3*, *NORE1A*, *p16INK4A*, *p14ARF*, *RASSF2A*, *SOCS1*, *RIZ1*, and *HOXB5*. Primer sequences and PCR conditions were described in a previous study [11]. PCR products were run on 2% agarose gels and visualized after staining with ethidium bromide.

2.4. Quantitative MSP analyses of RASSF1A, DCR2, and PCDHB family

Bisulfite-modified DNA was used as a template for TaqMan- or SYBR green I-based real-time PCR using a LightCycler (Roche Diagnostics), as described previously [11]. Primers and probes used to specifically amplify bisulfite-converted DNA for the internal reference gene (*ACTB*) and target genes (*RASSF1A*, *DCR2*, and *PCDHB family*) were described in Supplementary Table 1 [11,31]. Each amplification reaction included positive and negative controls for the methylation status of target genes, and tumor DNA samples with the bisulfite treatment. *ACTB* was used as a reference gene to determine the relative level of methylated DNA for one of the target genes in each sample.

We failed to detect quantitative PCR products using PCR primers and a probe for the exon 4 region of *CASP8*, from which PCR primer sequences for conventional PCR were obtained, probably because of low CpG contents of the region.

2.5. MYCN amplification analysis

DNA preparation, digestion, and Southern blot analysis using the *MYCN* probe were performed as described previously [34]. More than 3 copies of the *MYCN* gene per haploid genome were considered to indicate amplification.

2.6. Statistical analysis

The significance of differences in various biological and clinical aspects of the disease among the patient groups was examined by the Chi-square or Fisher's exact test. The Student's *t* test with or without Welch's correction compared the mean percentages of *RASSF1A*, *DCR2*, or *PCDHB* methylation between two types of tumors with or without *MYCN* amplification or any two ploidy groups classified by the age of patients and the method of tumor detection. The overall survival for each group of patients was estimated on August 30, 2003 by the Kaplan–Meier method, and compared using log-rank tests. The survival time was defined as the interval between remission induction or surgery and death from any cause. The influence of various biological and clinical factors on overall survival was estimated using the Cox proportional-hazards model calculated with Stat Flex software for Windows, version 6.0.

3. Results

3.1. Conventional and quantitative MSP analysis

The methylation status of *RASSF1A*, *CASP8*, *DCR2*, *HOXA9*, *RUNX3*, *NORE1A*, *p16INK4A*, *p14ARF*, *RASSF2A*, *SOCS1*, *RIZ1*, and *HOXB5* was examined using conventional MSP. Conventional MSP analysis of the *RASSF1A*, *CASP8*, and *DCR2* genes was performed in 259 neuroblastomas [123 found by mass-screening (group A1) and 136 found clinically (groups A2 + B)], and of the other 9 genes in 45 tumors (25 found by mass-screening and 20 diagnosed clinically). *RASSF1A*, *CASP8*, and *DCR2* were methylated in 57.7%, 3.3%, and 3.3% of 123 neuroblastomas found by mass-screening, in 51.6%, 10.9%, and 1.6% of 64 tumors diagnosed clinically (<18 months), and in 70.8%, 40.3%, and 38.9% of 72 tumors diagnosed clinically (>18 months) (Supplementary Tables 2–4). None of the 9 other genes (*HOXA9*, *RUNX3*, *NORE1A*, *p16INK4A*, *p14ARF*, *RASSF2A*, *SOCS1*, *RIZ1*, and *HOXB5*) were methylated in the 45 tumors.

Quantitative MSP analysis of *RASSF1A*, *DCR2*, and *PCDHB* methylation was carried out in 221 (85.3%), 116 (44.8%), and 116 (44.8%), respectively, of 259 neuroblastomas. Group A1 was included in *RASSF1A* analysis, and excluded from *DCR2* and *PCDHB* analysis. We performed ROC analysis, and determined cut-off values of 26%, 7%, and 18% of *RASSF1A*, *DCR2*, and *PCDHB* methylation (Fig. 1, A, B, and C). We then examined the dose–response relationship between percentages of *RASSF1A*, *DCR2* and *PCDHB* methylation (10%, 20%, 30%, 40%, 50%, 60%, 70% and 80%) and overall survival, and adopted the cut-off value of 40%, 70%, and 60%, respectively, which gave the highest HR (Fig. 1D–F). Although cut-off values were determined based on data of overall survival, they were also used for association analysis between gene methylation and clinical and *MYCN* features.

3.2. Correlation between RASSF1A, CASP8, DCR2, and PCDHB methylation and stage of the disease

We found no significant difference in stage distribution between *RASSF1A*-, *CASP8*-, and *DCR2*-methylated tumors and *RASSF1A*-, *CASP8*-, and *DCR2*-unmethylated tumors, respectively, determined by conventional MSP and found by mass-screening with an exception of *RASSF1A*-methylated diploid tumors (Table 1). *RASSF1A*-methylated tumors were at more advanced stages than *RASSF1A*-unmethylated tumors in infants and children diagnosed clinically ($P = 0.018$ and $P = 5.49E{-}05$). Quantitative MSP analysis confirmed the association. *CASP8*- and *DCR2*-methylated tumors were at a more advanced stage than *CASP8*- and *DCR2*-unmethylated tumors in children ($P = 0.026$ and $P = 5.06E{-}05$), however, such an association was not detected in tumors in infants diagnosed clinically. Quantitative MSP analysis of *DCR2* confirmed the association between the methylation and an advanced stage in children, but not in infants. The similar association was also found between *PCDHB*-methylated and –unmethylated tumors in children.

When tumors were further classified according to the ploidy status, *RASSF1A*-methylated diploid tumors were or were more likely to be a more advanced stage than *RASSF1A*-unmethylated diploid tumors in infants found by mass-screening ($P = 0.029$) or clinically diagnosed (<18 months) ($P = 0.052$) and in children (>18 months) ($P = 0.006$) (Table 1). *RASSF1A*-methylated triploid tumors in children were at a more advanced stage than *RASSF1A*-unmethylated triploid tumors in children ($P = 3.12E{-}03$), but not in infants found by mass-screening or clinically diagnosed. Quantitative MSP could not confirm the association in children.

Children with *CASP8*-methylated tumors were at a more advanced stage than those with *CASP8* unmethylated tumors in children ($P = 0.026$). *DCR2*-methylated diploid and triploid tumors in

Please cite this article in press as: M. Haruta et al., *RASSF1A* methylation may have two biological roles in neuroblastoma tumorigenesis depending on the ploidy status and age of patients, Cancer Lett. (2014), http://dx.doi.org/10.1016/j.canlet.2014.03.022

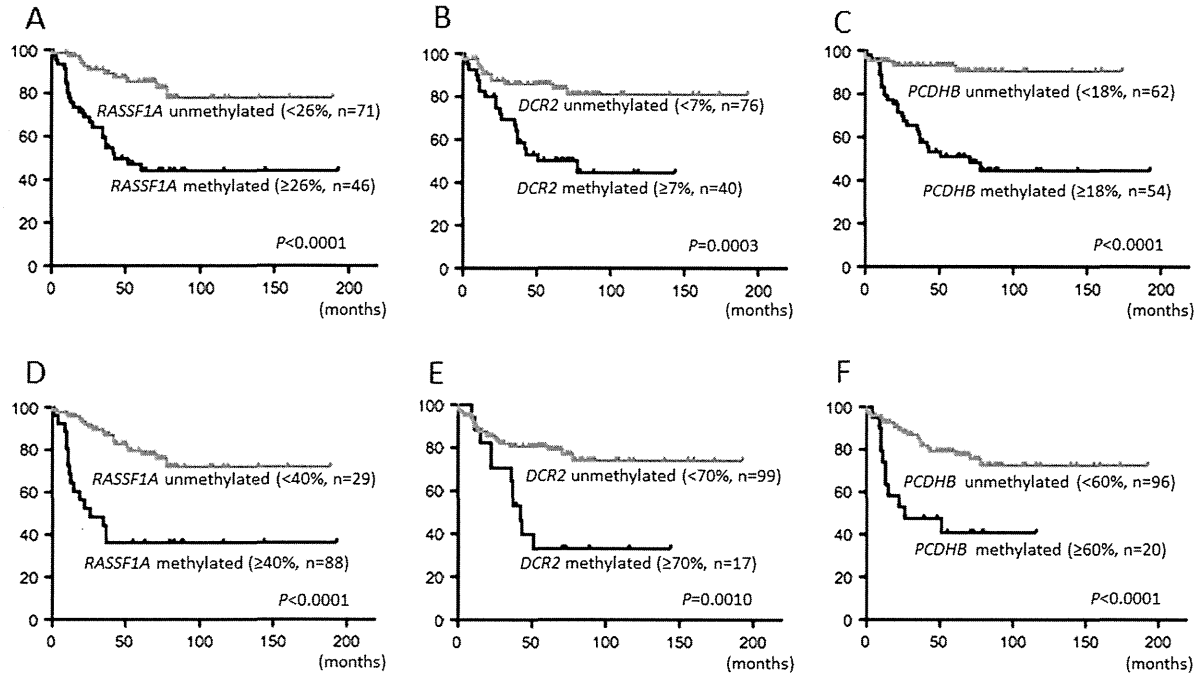

Fig. 1. Overall survival curves for infants and children diagnosed clinically and classified by the cut-off value in tumors determined by ROC analysis; (A) *RASSF1A*, 26% [$P < 0.0001$, hazard ratio (HR) 4.634, 95% confidence interval (95%CI) 2.3–9.3]; (B) *DCR2*, 7% ($P = 0.0003$, HR 3.91, 95%CI 1.9–8.2); (C) *PCDHB*, 18% ($P < 0.0001$, HR 5.35, 95%CI 2.7–10.8), and by the dose–response relationship; (D) *RASSF1A*, 40% ($P < 0.0001$, 7.89, 95%CI 3.3–19.2; (E) *DCR2*, 70% ($P = 0.001$, 5.34, 95%CI 2.0–14.5); (F) *PCDHB*, 60% ($P < 0.0001$, 6.11, 95%CI 2.2–16.9).

Table 1
Association between *RASSF1A*, *CASP8*, *DCR2*, and *PCDHB* methylation and stage of the disease.

	Group A1 (≤18 m)	Group A2 (≤18 m)	Group B (>18 m)		Group A2 (≤18 m)	Group B (>18 m)
RASSF1A (cMSP)				*RASSF1A* (qMSP)		
Total (methyl versus unmethyl)	NS	S (0.018)	S (5.49E−05)		ROC, S (0.029); DRR., NS	ROC, S (0.008); DRR., S (0.022)
Diploidy (methyl versus unmethyl)	S (0.029)	M (0.052)	S (0.006)		ROC, NS; DRR., NS	ROC, M (0.078); DRR., NS
Triploidy (methyl versus unmethyl)	NS	NS	S (3.12E−03)		ROC, NS; DRR, NA	ROC, M (0.080); DRR., NS
CASP8 (cMSP)						
Total (methyl versus unmethyl)	NS	M (0.090)	S (0.026)			
Diploidy (methyl versus unmethyl)	NA	NS	NS			
Triploidy (methyl versus unmethyl)	NS	NA	NS			
DCR2 (cMSP)				*DCR* (qMSP)		
Total (methyl versus unmethyl)	NS	NS	S (5.06E−05)		ROC, NS; DRR, NA.	ROC, S (0.005); DRR., S (0.004)
Diploidy (methyl versus unmethyl)	NS	NS	S (0.003)		ROC, NS; DRR, NA	ROC, M (0.057); DRR., S (0.033)
Triploidy (methyl versus unmethyl)	NS	NA	S (0.017)		ROC, NA ; DRR, NA	ROC, S (0.048); DRR., NS
PCDHB				*PCDHB* (qMSP)		
Total (methyl versus unmethyl)					ROC, NS; DRR., NS	ROC, S (5.70E−06); DRR., M (0.051)
Diploidy (methyl versus unmethyl)					ROC, NS; DRR., NS	ROC, S (0.001); DRR., NS
Triploidy (methyl versus unmethyl)					ROC, NS; DRR, NS	ROC, S (0.003); DRR., NS

Group A1, infants found by mass-screening; Group A2, infants diagnosed clinically; Group B, children diagnosed clinically; m, month; cMSP, conventional methylation-specific PCR; qMSP, quantitative methylation-specific PCR; Methyl, methylated; unmethyl, unmethylated; NS, not significant; S, significant; M, marginally significant; NA, not applicable; ROC, ROC analysis; DRR, dose–response relationship analysis; Detailed data are shown in Supplementary Tables 2–7.

Please cite this article in press as: M. Haruta et al., *RASSF1A* methylation may have two biological roles in neuroblastoma tumorigenesis depending on the ploidy status and age of patients, Cancer Lett. (2014), http://dx.doi.org/10.1016/j.canlet.2014.03.022

Table 2
Association between *RASSF1A*, *CASP8*, *DCR2*, and *PCDHB* methylation and *MYCN* amplification.

	Group A1 (≤18 m)	Group A2 (≤18 m)	Group B (>18 m)		Group A2 (≤18 m)	Group B (>18 m)
RASSF1A (cMSP)				*RASSF1A* (qMSP)		
Total (methyl versus unmethyl)	NS	S (0.001)	S (0.002)		ROC, S (5.29E−06); DRR., S (8.97E−06)	ROC, S (0.003); DRR., S (0.001)
Diploidy (methyl versus unmethyl)	NS	S (0.005)	S (0.011)		ROC, S (0.002); DRR., S (0.001)	ROC, S (0.003); DRR., S (0.003)
Triploidy (methyl versus unmethyl)	NA	NA	NS		ROC, NA; DRR., NA.	ROC, M (0.08); DRR, NS
CASP8 (cMSP)						
Total (methyl versus unmethyl)	NS	S (1.94E−07)	S (0.002)			
Diploidy (methyl versus unmethyl)	NA	S (1.35E−04)	S (0.034)			
Triploidy (methyl versus unmethyl)	NA	NA	S (0.027)			
DCR2 (cMSP)				*DCR2* (qMSP)		
Total (methyl versus unmethyl)	NS	NS	NS		ROC, S (0.043); DRR., NA	ROC, NS; DRR., NS
Diploidy (methyl versus unmethyl)	NS	NS	NS		ROC, NS; DRR., NA.	ROC, NS; DRR., NS
Triploidy (methyl versus unmethyl)	NA	NA	NS		ROC, NA; DRR., NA.	ROC, NS; DRR., NS
PCDHB (cMSP)				*PCDHB (qMSP)*		
Total (methyl versus unmethyl)					ROC, S (2.34E−07); DRR., S (1.2E−04)	ROC, S (0.003); DRR., M (0.091)
Diploidy (methyl versus unmethyl)					ROC, S (5.86E−06); DRR., S (0.005)	ROC, S (0.036); DRR., S (0.032)
Triploidy (methyl versus unmethyl)					ROC, NA; DRR, NA.	ROC, NS; DRR., NS

Group A1, infants found by mass-screening; Group A2, infants diagnosed clinically; Group B, children diagnosed clinically; m, month; cMSP, conventional methylation-specific PCR; qMSP, quantitative methylation-specific PCR; Methyl, methylated; unmethyl, unmethylated; NS, not significant; S, significant; M, marginally significant; NA, not applicable; ROC, ROC analysis; DRR, dose–response relationship analysis; Detailed data are shown in Supplementary Tables 2–7.

children were at a more advanced stage than *DCR2*-unmethylated diploid and triploid tumors in children, respectively ($P = 0.003$ and $P = 0.017$), and the results were consistent with those obtained by quantitative MSP.

Quantitative MSP analysis disclosed that *PCDHB*-methylated diploid and triploid tumors were at more advanced stages than *PCDHB*-unmethylated diploid and triploid tumors, respectively, in children ($P = 0.001$ and $P = 0.003$). Such an association was not found between *PCDHB*-methylated and -unmethylated tumors in infants.

3.3. Correlation of methylation in the RASSF1A, CASP8, DCR2, and PCDHB genes with MYCN amplification

Because only 2 of 123 tumors found by mass-screening had *MYCN* amplification, further studies on the correlation were not conducted (Table 2). *RASSF1A* methylation detected by conventional MSP was associated with *MYCN* amplification in tumors in infants and children ($P = 0.001$ and $P = 0.002$). *CASP8* methylation was also associated with *MYCN* amplification in tumors in infants and children ($P = 1.94E{-}07$ and $P = 0.002$). In contrast, no association was found between *DCR2* methylation and *MYCN* amplification in tumors in infants and children. Quantitative MSP analysis in *RASSF1A* and *DCR2* methylation confirmed the findings. In addition, *PCDHB* methylation was also identified to have correlation with *MYCN* amplification in tumors of infants and children. The association between *RASSF1A* and *PCDHB* methylation and *MYCN* amplification was also indicated by different distributions of methylation percentages of *RASSF1A* and *PCDHB* between *MYCN*-amplified and –nonamplified tumors; however, different distributions of *DCR2* methylation percentages were not exhibited between the tumors in infants and children (Fig. 2).

We then classified tumors by the ploidy status, and found that none of the triploid tumors in infants had *MYCN* amplification. *RASSF1A* methylation was associated with *MYCN* amplification in diploid tumors in infants and children ($P = 0.005$ and $P = 0.011$), but not in triploid tumors in children. *DCR2* methylation was not associated with *MYCN* amplification in diploid and triploid tumors in children. Quantitative MSP analysis confirmed the association with *MYCN* amplification found in *RASSF1A*-methylated tumors, and no association found in *DCR2*-methylated tumors. *CASP8* methylation was associated with *MYCN* amplification in diploid tumors in infants ($P = 1.35E{-}04$) or in diploid and triploid tumors in children ($P = 0.034$ and $P = 0.027$). The correlation between *PCDHB* methylation and *MYCN* amplification was found in tumors of infants and children. When divided by the ploidy status, *RASSF1A* and *PCDHB* methylation was correlated with *MYCN* amplification in diploid, not triploid tumors in infants and children. *DCR2* methylation (>7%) was found only 3 of 53 tumors in infants; further study was not conducted. The correlation between *DCR2* methylation and *MYCN* amplification was not found in tumors of children.

3.4. Correlation between the methylation status of the RASSF1A, CASP8, DCR2, and PCDHB genes analyzed by conventional and quantitative MSP and overall survival

There was no prognostic significance of methylation of *RASSF1A*, *CASP8*, and *DCR2* in infants found by mass-screening because only two of 123 infants died of the disease (Table 3 and Supplementary Tables 2–4). When we combined infants and children clinically

Please cite this article in press as: M. Haruta et al., *RASSF1A* methylation may have two biological roles in neuroblastoma tumorigenesis depending on the ploidy status and age of patients, Cancer Lett. (2014), http://dx.doi.org/10.1016/j.canlet.2014.03.022

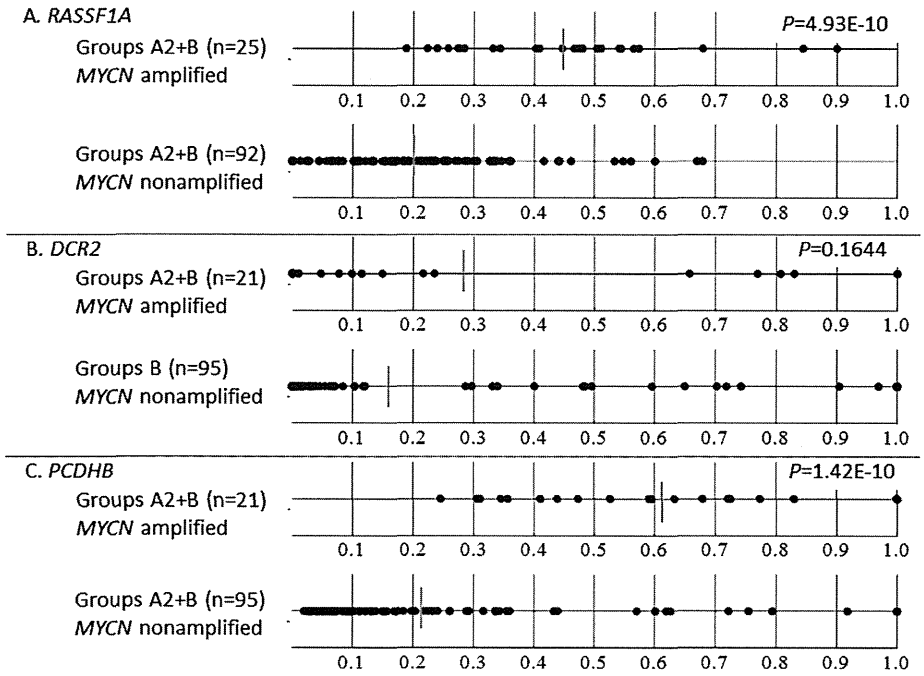

Fig. 2. The distribution of *RASSF1A*, *DCR2*, and *PCDHB* methylation percentages between *MYCN* amplified and *MYCN*-nonamplified tumors.

Table 3
Association between *RASSF1A*, *CASP8*, *DCR2*, and *PCDHB* methylation and overall survival.

	Group A1 (≤18 m)	Group A2 (≤18 m)	Group B (>18 m)		Group A2 (≤18 m)	Group B (>18 m)
RASSF1A (cMSP)				*RASSF1A* (qMSP)		
Total (methyl versus unmethyl)	NS	M (0.0705)	S (0.0331)		ROC, S (0.0001); DRR., S (0.0002)	ROC, S (0.0288); DRR., S (0.0060)
Diploidy (methyl versus unmethyl)	NS	S (0.0405)	NS		ROC, S (0.0057); DRR., S (0.0031)	ROC, NS; DRR., NS
Triploidy (methyl versus unmethyl)	NA	NS	NS		ROC, NA; DRR., NA	ROC, NS; DRR., S (0.0126)
CASP8 (cMSP)						
Total (methyl versus unmethyl)	NS	S (<0.0001)	NS			
Diploidy (methyl versus unmethyl)	NA	S (0.0027)	NS			
Triploidy (methyl versus unmethyl)	NA	NA	NS			
DCR2 (cMSP)				*DCR2* (qMSP)		
Total (methyl versus unmethyl)	NS	NA	M (0.0821)		ROC, S (0.0020); DRR., NA	ROC, NS; DRR., S (0.0360)
Diploidy (methyl versus unmethyl)	NA	NA	NS		ROC, S (0.0381); DRR., NA	ROC, NS; DRR., NS
Triploidy (methyl versus unmethyl)	NA	NA	S (0.0182)		ROC, NA; DRR., NA	ROC, NS; DRR., S (0.0164)
PCDHB (cMSP)				*PCDHB* (qMSP)		
Total (methyl versus unmethyl)					ROC, S (0.0101); DRR., S (<0.0001)	ROC, S (0.0218); DRR., NS
Diploidy (methyl versus unmethyl)					ROC, M (0.0609); DRR., S (0.0007)	ROC, NS; DRR., S (0.0451)
Triploidy (methyl versus unmethyl)					ROC, NA; DRR., NA	ROC, M (0.0850); DRR., NS

Group A1, infants found by mass-screening; Group A2, infants diagnosed clinically; Group B, children diagnosed clinically; m, month; cMSP, conventional methylation-specific PCR; qMSP, quantitative methylation-specific PCR; Methyl, methylated; unmethyl, unmethylated; NS, not significant; S, significant; M, marginally significant; NA, not applicable; ROC, ROC analysis; DRR, dose–response relationship analysis; Detailed data are shown in Supplementary Tables 2–7.

diagnosed, patients with a *RASSF1A*-, *CASP8*-, or *DCR2*-methylated tumor examined by conventional MSP had worse overall survival than patients with a *RASSF1A*-, *CASP8*-, or *DCR2*-unmethylated tumor, respectively ($P = 0.0015$, $P = 0.0003$, and $P = 0.0038$) (Fig. 3A–C).

When we further classified patients according to the ploidy status, infants with a *RASSF1A*-methylated diploid tumor had worse overall survival than infants with a *RASSF1A*-unmethylated diploid tumor ($P = 0.0405$); however, such an association was not found in infants with triploid tumors (Fig. 3D and F). In addition, infants with a *CASP8*-methylated diploid tumor had worse overall survival than infants with a *CASP8*-unmethylated diploid tumor ($P = 0.0027$). No significant difference was observed in overall

Please cite this article in press as: M. Haruta et al., *RASSF1A* methylation may have two biological roles in neuroblastoma tumorigenesis depending on the ploidy status and age of patients, Cancer Lett. (2014), http://dx.doi.org/10.1016/j.canlet.2014.03.022

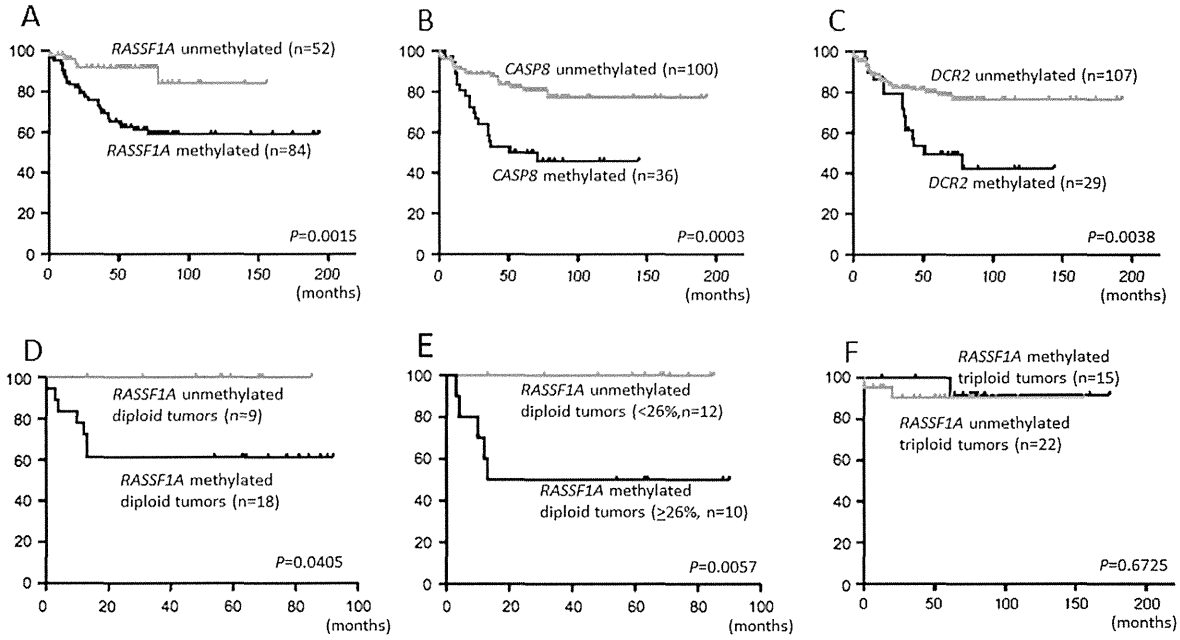

Fig. 3. Overall survival curves for infants and children diagnosed clinically and classified by the methylation status of *RASSF1A* (A), *CASP8* (B), and *DCR2* (C) examined by conventional MSP analysis. Overall survival curves for infants with a *RASSF1A*-methylated diploid tumor and those with a *RASSF1A*-unmethylated diploid tumor diagnosed clinically and examined by conventional MSP (D), or quantitative MSP (E) analysis, and for infants with a *RASSF1A*-methylated triploid tumor and those with a *RASSF1A*-unmethylated triploid tumor diagnosed clinically and examined by conventional MSP (F).

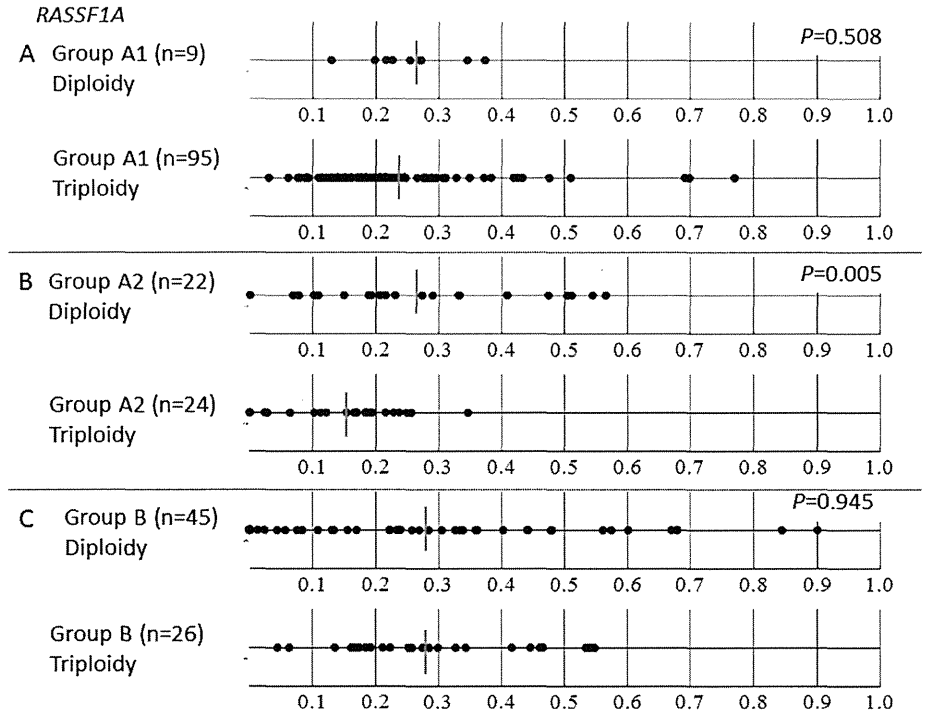

Fig. 4. The distribution of *RASSF1A* methylation percentages between diploid and triploid tumors in infants found by mass-screening (A), between diploid and triploid tumors in infants (<18 months) diagnosed clinically (B), and between diploid and triploid tumors in children (>18 months) (C).

survival between any two of the 4 types of tumors classified by the methylation status of *RASSF1A* or *CASP8* and the ploidy status in children. In contrast, children with a *DCR2*-methylated triploid tumor had worse overall survival than children with a *DCR2*-unmethylated triploid tumor ($P = 0.0182$).

When we analyzed *RASSF1A*, *DCR2*, and *PCDHB* methylation by quantitative MSP, an association between methylation of each gene and poor outcomes was identified in tumors of infants and children (Table 3). When we divided tumors according to the ploidy status, *RASSF1A* and *DCR2*, not *PCDHB* methylation was associated with a poor outcome in infants with a diploid, not triploid tumor. Interestingly, *RASSF1A* and *DCR2* methylation was correlated with a poor outcome in children with a triploid, not diploid tumor.

Please cite this article in press as: M. Haruta et al., *RASSF1A* methylation may have two biological roles in neuroblastoma tumorigenesis depending on the ploidy status and age of patients, Cancer Lett. (2014), http://dx.doi.org/10.1016/j.canlet.2014.03.022

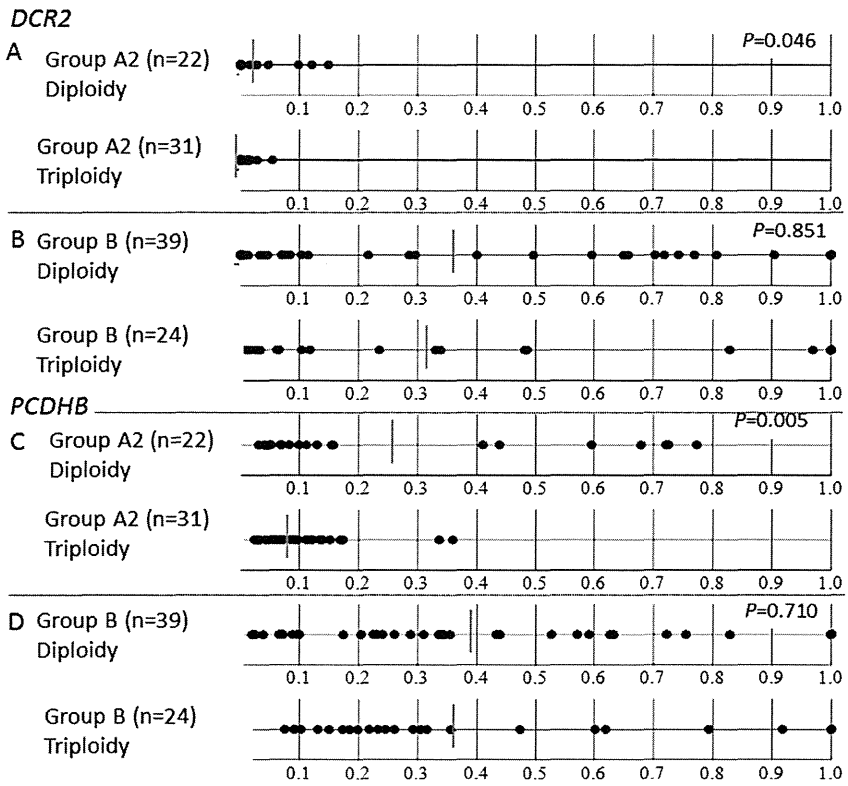

Fig. 5. The distribution of *DCR2* methylation percentages between diploid and triploid tumors in infants (<18 months) diagnosed clinically (A), and between diploid and triploid tumors in children (>18 months) (B). The distribution of *PCDHB* methylation percentages between diploid and triploid tumors in infants (<18 months) diagnosed clinically (C), and between diploid and triploid tumors in children (>18 months) (D).

Table 4
Multivariate analysis on 5 clinicopathological and genetic factors including *RASSF1A* methylation in 102 patients with neuroblastoma.

Prognostic factors	Relative risk (95%CI[a])	*P*-value	Relative risk (95%CI[a])	*P*-value
Age: ≤18 months versus > 18 months	2.07 (0.84–5.13)	0.1159	1.88 (0.75–4.70)	0.1754
Stage: 1, 2, 4S versus 3, 4	2.71 (0.79–9.27)	0.1116	2.88 (0.86–9.62)	0.0859
Ploidy: Triploidy versus diploidy	1.40 (0.65–3.01)	0.3940	1.26 (0.58–2.75)	0.5648
MYCN: Single copy versus amplification	3.19 (1.45–7.03)	0.0041	3.30 (1.55–7.00)	0.0019
RASSF1A [b]: Unmethylated (<26%) versus methylated (>26%)	1.55 (0.67–3.61)	0.3086		
RASSF1A [c]: Unmethylated (<40%) versus methylated (>40%)			2.19 (1.02–4.72)	0.0455

[a] 95%CI, 95% confidence interval.
[b] The cut-off value was determined by ROC analysis.
[c] The cut-off value was determined by the dose-response relationship.

3.5. The mean methylation percentage between diploid and triploid tumors in infants and children

The mean methylation percentage of *RASSF1A* was higher in diploid tumors than in triploid tumors of infants diagnosed clinically; however, such an association was not observed in tumors of infants found by mass-screening or children (Fig. 4). Likewise, the mean methylation percentage of *DCR2* or *PCDHB* was higher in diploid tumors than in triploid tumors of infants; however, such an association was not observed between diploid and triploid tumors in children (Fig. 5).

The difference in the methylation percentage of *RASSF1A* or *DCR2* between diploid and triploid tumors in infants, but not in children reflected the difference in outcomes between infants having a diploid tumor with or without *RASSF1A* or *DCR2* methylation ($P = 0.0057$ and $P = 0.0381$), but not between children having a diploid tumor with or without (Table 3). Interestingly, the difference in outcomes was observed between children having a triploid tumor with or without *RASSF1A* or *DCR2* methylation, but not between infants having a triploid tumor with or without; methylation percentages of *RASSF1A* or *DCR2* rarely exceeded cut-off values of 27% or 7% in triploid tumors in infants (Figs. 4 and 5).

3.6. Multivariate Cox proportional hazard regression analysis on 5 clinical and genetic factors in 102 patients clinically diagnosed

Multivariate analysis exhibited the *MYCN* amplification and *RASSF1A* methylation statuses were shown to be independent factors predicting poor outcome, but the *PCDHB* and *DCR2* methylation statuses were not (Table 4, and Supplementary Tables 8 and 9).

4. Discussion

The present study using conventional MSP found methylation of the *RASSF1A*, *CASP8*, and *DCR2* genes in 62%, 25%, and 21%, respectively, of 136 neuroblastoma samples diagnosed clinically. Previous studies reported methylation of *RASSF1A*, *CASP8*, and *DCR2* in

Please cite this article in press as: M. Haruta et al., *RASSF1A* methylation may have two biological roles in neuroblastoma tumorigenesis depending on the ploidy status and age of patients, Cancer Lett. (2014), http://dx.doi.org/10.1016/j.canlet.2014.03.022

Table 5
Incidences and associations between *RASSF1A*, *CASP8*, and *DCR2* methylation and disease stage, *MYCN* amplification, and overall or event-free survival.

Studies	*RASSF1A*				*CASP8*				*DCR2*			
	Incidence	Stage	*MYCN* amp.	Survival	Incidence	Stage	*MYCN* amp.	Survival	Incidence	Stage	*MYCN* amp.	Survival
Astuti et al. [14]	55%, 37/67	N. S.	N. S.	N. S.	40%, 24/60	N. D.	N. D.	N. D.				
Yang et al. [15]	70%, 39/56	N. S.	N. S.	OS, $P < 0.01$								
Banelli et al. [16]	84%, 26/31	N. D.	$P < 0.05$	OS, N. S.		N. D.	N. S.	N. D.	42%, 13/31	N. D.	N. S.	OS, $P < 0.03$
Lázcoz et al. [17]	83%, 29/35	N. D.	N. S.	N. D.	60%, 21/35	N. D.	N. S.	N. D.				
Yang et al. [18]	90%, 63/70	N. D.	N. D.	N. D.	56%, 39/70	N. D.	N. S.	OS, $P = 0.008$	44%, 31/70	N. D.	N. D.	OS, $P = 0.019$
Michalowski et al. [19]	93%, 42/45	N. D.	N. D.	N. S.	38%, 17/45	$P = 0.001$	N. S.	N. S.				
Misawa et al. [20]	94%, 64/68	N. S.	N. S.	N. S.								
Hoebeeck et al. [21]	71%, 29/41	N. S.	N. S.	OS and EFS, N. S.	56%, 20/36	N. S.	N. S.	EFS, $P = 0.038$				
Grau et al. [22]	66%, 54/82	$P = 0.024$	N. S.	EFS, $P = 0.003$ (intermediate risk)	52%, 43/8	$P < 0.001$	$P = 0.007$	OS, $P = 0.019$ EFS, $P = 0.002$				
Stutterheim et al. [23]	96%, 68/71	N. D.	St 1–3, $P = 0.006$ St 4, $P = 0.05$	OS, $P = 0.02$ (St 4 & > 1 y.)								
Kiss et al. [24]	61%, 23/38	N. D.	N. D.	N. D.	55%, 21/38	N. D.	N. S.	N. D.				
Teitz et al. [25]					62%, 26/42	N. S.	$P < 0.0001$	N. D.				
Takita et al. [26]					32%, 8/25	N. D.	N. S.	N. D.				
Gonzalez-Gomez et al. [27]					14%, 6/38	$P = 0.019$	$P = 0.0047$	N. D.				
Asada et al. [28]					19%, 26/140 20%, 30/152	N. D.	N. D.	OS $P = 0.002$ in Japanese $P = 0.0002$ in German				
van Noesel et al. [29]									70%, 39/56	N. D.	N. D.	N. D.
Yagyu et al. [30]									28%, 24/86	N. D.	N. D.	OS, $P = 0.008$ EFS, $P < 0.001$
Present study	62%, 84/136	<18 m, $P = 0.018$ >18 m, $P < 0.001$	$P < 0.001$	OS, $P = 0.0015$	27%, 36/136	<18 m $P = 0.090$ >18 m $P = 0.026$	$P = 0.0003$	OS, $P < 0.001$	21%, 29/136	<18 m, $P = 0.406$ >18 m, $P < 0.001$	$P = 0.149$	OS, $P = 0.0038$

N. S., not significant; N. D., not done; OS, overall survival; EFS, event-free survival; st, stage; 1 y., one year; Studies were cited in the Reference section.

55–96%, 14–62%, and 28–70% in 25–86 neuroblastoma samples (Table 5) [14–30]. The various results may have been affected by the location of primers for target genes and numbers of PCR cycles used for conventional and quantitative MSP analysis. We also evaluated *PCDHB* methylation, which was reported in a substantial number of neuroblastoma samples [31].

Regarding to methylation of the 4 genes and the stage distribution, *RASSF1A* methylation was associated with a more advanced stage in infants and children diagnosed clinically and in infants with a diploid tumor found by mass-screening, whereas *CASP8*, *DCR2*, and *PCDHB* methylation was associated with an advanced stage only in tumors of children (Table 1). The findings reflected that *RASSF1A* methylation was fairly common in neuroblastoma in infants, while *CSAP8*, *DCR2*, and *PCDHB* methylation was rare in tumors of infants, especially in triploid tumors.

Associations between *RASSF1A*, or *CASP8* methylation and *MYCN* amplification have been reported (Table 5) [14–28]. In addition, neuroblastoma with *PCDHB* methylation was reported to include all tumors with *MYCN* amplification, and associated with a poor outcome [31]. The present study exhibited that *RASSF1A*, *CASP8*, or *PCDHB* methylation was correlated with *MYCN* amplification in tumors of infants and children, but *DCR2* methylation was not (Table 2 and Fig. 2). Based on classification by the ploidy status, the association between *RASSF1A* or *PCDHB* methylation and *MYCN* amplification was observed in diploid tumors of infants and children; triploid tumors in infants had no *MYCN* amplification, therefore, associations could not be examined. *CASP8* methylation was associated with *MYCN* amplification in diploid tumors of infants and children, and triploid tumors in children.

Regarding to overall survival, the present study using conventional and/or quantitative MSP analysis exhibited association between *RASSF1A*, *DCR2*, and *PCDHB* methylation and poor outcomes in infants and children (Table 3 and Fig. 1), especially in diploid tumors of infants, and triploid tumors of children; *CASP8* methylation was only associated with a poor outcome in infants with a diploid tumor. Thus, *RASSF1A* methylation was associated with at a more advanced stage, *MYCN* amplification, and a poor outcome in infants with a diploid tumor. Although a substantial number of triploid tumors in infants exhibited *RASSF1A* methylation by conventional MSP analysis, they had no *MYCN* amplification and showed a favorable outcome, suggesting triploid tumors in infants as a specific biological subtype of neuroblastoma. Children with *RASSF1A*-, *DCR2*-, and *PCDHB*-methylated tumors had poorer outcomes than children with *RASSF1A*-, *DCR2*-, and *PCDHB*-unmethylated tumors, respectively. The association between *RASSF1A* and *DCR2* methylation and a poor outcome in children with triploid tumors is noteworthy, because the association was also observed in infants having a diploid tumor with or without *RASSF1A* and *DCR2* methylation. These findings suggest 2 subtypes of triploid neuroblastoma; while one was common in infants, exhibited hypomethylation of *RASSF1A* and *DCR2*, no *MYCN* amplification, and a favorable outcome, the other was common in children, exhibited hypermethylation of *RASSF1A*, *DCR2*, and *PCDHB*, frequent *MYCN* amplification, and an unfavorable outcome. We previously stated that triploidy in infant neuroblastoma may arisen through tetraploidization and succeeding tripolar division, whereas triploidy in childhood neuroblastoma may have derived from tetraploidization and chromosome loss [36]. We suggest that different mechanisms of triploid formation may have contributed to the different epigenetic features between infant and childhood triploid tumors. INRG proposed that patients with a hyperdiploid tumor be classified at low risk, whereas patients with a diploid tumor be classified at intermediate risk if they were $\leqslant$18 months of age and at the distantly metastatic stage [33]. We provided the data on epigenetic differences between diploid and triploid tumors in infants, and supported the inclusion of the ploidy status as one of factors included in the INRG classification system.

A recent study proposed a model in which the binding of TNFα to the death receptor, TNFαR1 results in its internalization, and subsequent formation of a complex with MOAP-1/RASSF1A to promote the open form of MOAP-1 to associate with Bax. This in turn results in Bax conformational changes and recruitment to the mitochondria to initiate cell death [10]. Silencing of *RASSF1A* due to promoter methylation by DNMT3B facilitated by MYCN and PRC2 was shown to avoid neuroblastoma cells entering apoptosis [37]. Thus, we consider that *RASSF1A*-methylated diploid tumors avoid entering apoptosis, facilitate proliferation, and finally cause unfavorable outcomes in infants and children with overexpressed MYCN with or without *MYCN* amplification.

On the other hand, aneuploidy has been shown to cause a proliferative disadvantage in yeast because of the overexpression of certain metabolism-associated genes [38], and it has been speculated that hypermethylation of the promoter regions of genes in cancer cells may lessen the metabolic impact of aneuploidy by silencing genes on a supernumerary chromosome while preserving the expression of other genes on chromosome that confer a selective advantage [39]. We propose that *RASSF1A* methylation in triploid neuroblastomas in infants found by mass-screening or diagnosed clinically may modulate their expression levels to repress cell cycle arrest and microtubule stabilization.

DCR2 is an antiapoptotic decoy receptor, which disturbs TRAIL-induced apoptosis in normal cells [29]. The present findings showing that *MYCN* amplification was associated with *RASSF1A*, *CASP8*, and *PCDHB* methylation, but not with *DCR2* methylation, may be explained by the transcriptional regulation of MYCN to the *RASSF1A*, *CASP8*, and *PCDHB* promoters, but not to the *DCR2* promoter.

In conclusion, the present study disclosed 2 subtypes of triploid neurblastoma with different clinical and epigenetic characteristics. These findings will facilitate understanding of heterogeneous biology of neuroblastoma, and improve choice of the treatment.

Conflict of interest

None.

Appendix A. Supplementary material

Supplementary data associated with this article can be found, in the online version, at http://dx.doi.org/10.1016/j.canlet.2014.03.022.

References

[1] J.M. Maris, M.D. Hogarty, R. Bagatell, S.L. Cohn, Neuroblastoma, Lancet 369 (2007) 2106–2115.
[2] G.M. Brodeur, Neuroblastoma: biological insights into a clinical enigma, Nat. Rev. Cancer 3 (2003) 203–216.
[3] M. Schwab, F. Westermann, B. Hero, F. Berthold, Neuroblastoma: biology and molecular and chromosomal pathology, Lancet Oncol. 4 (2003) 472–480.
[4] T. Sawada, M. Hirayama, T. Nakata, T. Takeda, N. Takasugi, T. Mori, et al., Mass screening for neuroblastoma in infants in Japan, Lancet 2 (1984) 271–273.
[5] W.G. Wood, R.N. Gao, J.J. Shuster, L.L. Robison, M. Bernstin, S. Weitzman, et al., Screening of infants and mortality due to neuroblastoma, N. Engl. J. Med. 346 (2002) 1041–1046.
[6] F.H. Schilling, C. Spix, F. Berthold, R. Erttmann, N. Fehse, B. Hero, et al., Neuroblastoma screening at one year of age, N. Engl. J. Med. 346 (2002) 1047–1053.
[7] E. Hiyama, T. Iehara, T. Sugimoto, M. Fukuzawa, Y. Hayashi, F. Sasaki, et al., Effectiveness of screening for neuroblastoma at 6 months of age: a retrospective population-based cohort study, Lancet 371 (2008) 1173–1180.
[8] A. Agathanggelou, W.N. Cooper, F. Latif, Role of the Ras-association domain family 1 tumor suppressor gene in human cancer, Cancer Res. 65 (2005) 3497–3508.
[9] A.M. Richter, G.P. Pfeifer, R.H. Dammann, The RASSF proteins in cancer; from epigenetic silencing to functional characterization, Biochim. Biophys. Acta 1796 (2009) 114–128.

Please cite this article in press as: M. Haruta et al., *RASSF1A* methylation may have two biological roles in neuroblastoma tumorigenesis depending on the ploidy status and age of patients, Cancer Lett. (2014), http://dx.doi.org/10.1016/j.canlet.2014.03.022

[10] M. Gordon, S. Baksh, RASSF1A: not a prototypical Ras effector, Small GTPases 2 (2011) 148–157.
[11] S. Honda, M. Haruta, W. Sugawara, F. Sasaki, M. Ohira, T. Matsunaga, et al., The methylation status of *RASSF1A* promoter predicts responsiveness to chemotherapy and eventual cure in hepatoblastoma patients, Int. J. Cancer 123 (2008) 1117–1125.
[12] J. Wang, B. Wang, X. Chen, J. Bi, The prognostic value of RASSF1A promoter hypermethylation in non-small cell lung carcinoma: a systematic review and meta-analysis, Carcinogenesis 32 (2011) 441–446.J.
[13] J. Ohshima, M. Haruta, Y. Fujiwara, N. Watanabe, Y. Arai, T. Ariga, et al., Methylation of the *RASSF1A* promoter is predictive of poor outcome among patients with Wilms tumor, Ped. Blood Cancer 59 (2012) 499–505.
[14] D. Astuti, A. Agathanggelou, S. Honorio, A. Dallol, T. Martinsson, P. Kogner, et al., *RASSF1A* promoter region CpG island hypermethylation in phaeochromocytomas and neuroblastoma tumours, Oncogene 20 (2001) 7573–7577.
[15] Q. Yang, P. Zage, D. Kagan, Y. Tian, R. Seshadri, H.R. Salwen, et al., Association of epigenetic inactivation of *RASSF1A* with poor outcome in human neuroblastoma, Clin. Cancer Res. 10 (2004) 8493–8500.
[16] B. Banelli, I. Gelvi, A. Di Vinci, P. Scaruffi, I. Casciano, G. Allemanni, et al., Distinct CpG methylation profiles characterize different clinical groups of neuroblastic tumors, Oncogene 24 (2005) 5619–5628.
[17] P. Lázcoz, J. Muñoz, M. Nistal, A. Pestaña, I. Encío, J.S. Castresana, Frequent promoter hypermethylation of RASSF1A and CASP8 in neuroblastoma, BMC Cancer 6 (2006) 254–264.
[18] Q. Yang, C.M. Kiernan, Y. Tian, H.R. Salwen, A. Chlenski, B.A. Brumback, et al., Methylation of *CASP8*, *DCR2*, and *HIN-1* in neuroblastoma is associated with poor outcome, Clin. Cancer Res. 13 (2007) 3191–3197.
[19] M.B. Michalowski, F. Fraipont, D. Plantaz, S. Michelland, V. Combaret, M.C. Favrot, Methylation of tumor-suppressor genes in neuroblastoma: the RASSF1A gene is almost always methylated in primary tumors, Ped. Blood Cancer 50 (2008) 29–32.
[20] A. Misawa, S. Tanaka, S. Yagyu, K. Tsuchiya, T. Iehara, T. Sugimoto, et al., *RASSF1A* hypermethylation in pretreatment serum DNA of neuroblastoma patients: a prognostic marker, Br. J. Cancer 100 (2009) 399–404.
[21] J. Hoebeeck, E. Michels, F. Pattyn, V. Combaret, J. Vermeulen, N. Yigit, et al., Aberrant methylation of candidate tumor suppressor genes in neuroblastoma, Cancer Lett. 273 (2009) 336–346.
[22] E. Grau, F. Martinez, C. Orellana, A. Canete, Y. Yañez, S. Oltra, et al., Hypermethylation of apoptotic genes as independent prognostic factor in neuroblastoma disease, Mol Carcinog. 50 (2011) 153–162.
[23] J. Stutterheim, F.A. Ichou, E. Ouden, R. Versteeg, H.N. Caron, G.A. Tytgat, et al., Methylated RASSF1a is the first specific DNA marker for minimal residual disease testing in neuroblastoma, Clin. Cancer Res. 18 (2012) 808–814.
[24] N.B. Kiss, P. Kogner, J.I. Johnsen, T. Martinsson, C. Larsson, J. Geli, Quantitative global and gene-specific promoter methylation in relation to biological properties of neuroblastomas, BMC Med. Genet. (2012), http://dx.doi.org/10.1186/1471-2350-13-83.
[25] T. Teitz, T. Wei, M.B. Valentine, E.F. Vanin, J. Grenet, V.A. Valentine, et al., Caspase 8 is deleted or silenced preferentially in childhood neuroblastomas with amplification of *MYCN*, Nat. Med. 6 (2000) 529–535.
[26] J. Takita, H.W. Yang, Y.Y. Chen, R. Hanada, K. Yamamoto, T. Teitz, et al., Allelic imbalance on chromosome 2q and alterations of the caspase 8 gene in neuroblastoma, Oncogene 20 (2001) 4424–4432.
[27] P. Gonzalez-Gomez, M.J. Bello, J. Lomas, D. Arjona, M.E. Alonso, C. Amiñoso, et al., Aberrant methylation of multiple genes in neuroblastic tumours: relationship with *MYCN* amplification and allelic status at 1p, Eur. J. Cancer 39 (2003) 1478–1485.
[28] K. Asada, N. Watanabe, Y. Nakamura, M. Ohira, F. Westermann, M. Schwab, A. Nakagawara, T. Ushijima, Stronger prognostic power of the CpG island methylator phenotype than methylation of individual genes in neuroblastomas, Jpn. J. Clin. Oncol. 43 (2013) 641–645.
[29] M.M. van Noesel, S. Bezouw, G.S. Salomons, P.A. Voûte, R. Pieters, S.B. Baylin, et al., Tumor-specific down-regulation of the tumor necrosis factor-related apoptosis-inducing ligand decoy receptors DcR1 and DcR2 is associated with dense promoter hypermethylation, Cancer Res. 62 (2002) 2157–2161.
[30] S. Yagyu, T. Gotoh, T. Iehara, M. Miyachi, Y. Katsumi, S. Tsubai-Shimizu, et al., *Circulating methylated-DCR2 gene in serum as an indicator of prognosis and* therapeutic efficacy in patients with *MYCN* nonamplified neuroblastoma, Clin. Cancer Res. 14 (2008) 7011–7019.
[31] M. Abe, M. Ohira, A. Kaneda, Y. Yagi, S. Yamamoto, Y. Kitano, T. Takato, A. Nakagawara, T. Ushijima, CpG island methylator phenotype is a strong determinant of poor prognosis in neuroblastomas, Cancer Res. 65 (2005) 828–834.
[32] Y. Kaneko, H. Kobayashi, N. Watanabe, N. Tomioka, A. Nakagawara, Biology of neuroblastomas that were found by mass screening at 6 months of age in Japan, Ped. Blood Cancer 46 (2006) 285–291.
[33] S.L. Cohn, A.D. Pearson, W.B. London, T. Monclair, P.F. Ambros, G.M. Brodeur, et al., The International Neuroblastoma Risk Group (INRG) classification system: an INRG task force report, J. Clin. Oncol. 27 (2009) 289–297.
[34] Y. Kaneko, H. Kobayashi, N. Maseki, A. Nakagawara, M. Sakurai, Disomy 1 with terminal 1p deletion was frequent in mass screening-negative/late-presenting neuroblastomas in young children, but not in mass screening-positive neuroblastomas in infants, Int. J. Cancer 80 (1999) 54–59.
[35] J.G. Herman, J.R. Graff, S. Myöhänen, B.D. Nelkin, S.B. Baylin, Methylation-specific PCR: a novel PCR assay for methylation status of CpG islands, Proc. Natl. Acad. Sci. USA 93 (1996) 9821–9826.
[36] Y. Kaneko, A.G. Knudson, Mechanism and relevance of ploidy in neuroblastoma, Genes Chromosomes Cancer 29 (2000) 89–95.
[37] R.K. Palakurthy, N. Wajapeyee, M.K. Santra, C. Gazin, L. Lin, S. Gobeil, et al., Epigenetic silencing of the *RASSF1A* tumor suppressor gene through HOXB3-mediated induction of *DNMT3B* expression, Mol. Cell 36 (2009) 219–230.
[38] T. Galitski, A.J. Saldanha, C.A. Styles, E.S. Lander, G.R. Fink, Ploidy regulation of gene expression, Science 285 (1999) 251–254.
[39] P.V. Jallepalli, D. Pellman, Cell biology. Aneuploidy in the balance, Science 317 (2007) 904–905.

Please cite this article in press as: M. Haruta et al., *RASSF1A* methylation may have two biological roles in neuroblastoma tumorigenesis depending on the ploidy status and age of patients, Cancer Lett. (2014), http://dx.doi.org/10.1016/j.canlet.2014.03.022

Published OnlineFirst May 15, 2014; DOI: 10.1158/0008-5472.CAN-14-0241

Molecular and Cellular Pathobiology

Cancer Research

Flotillin-1 Regulates Oncogenic Signaling in Neuroblastoma Cells by Regulating ALK Membrane Association

Arata Tomiyama[1,3], Takamasa Uekita[1,4], Reiko Kamata[1], Kazuki Sasaki[5], Junko Takita[2], Miki Ohira[6], Akira Nakagawara[7], Chifumi Kitanaka[8], Kentaro Mori[3], Hideki Yamaguchi[1], and Ryuichi Sakai[1]

Abstract

Neuroblastomas harbor mutations in the nonreceptor anaplastic lymphoma kinase (ALK) in 8% to 9% of cases where they serve as oncogenic drivers. Strategies to reduce ALK activity offer clinical interest based on initial findings with ALK kinase inhibitors. In this study, we characterized phosphotyrosine-containing proteins associated with ALK to gain mechanistic insights in this setting. Flotillin-1 (FLOT1), a plasma membrane protein involved in endocytosis, was identified as a binding partner of ALK. RNAi-mediated attenuation of FLOT1 expression in neuroblastoma cells caused ALK dissociation from endosomes along with membrane accumulation of ALK, thereby triggering activation of ALK and downstream effector signals. These features enhanced the malignant properties of neuroblastoma cells *in vitro* and *in vivo*. Conversely, oncogenic ALK mutants showed less binding affinity to FLOT1 than wild-type ALK. Clinically, lower expression levels of FLOT1 were documented in highly malignant subgroups of human neuroblastoma specimens. Taken together, our findings suggest that attenuation of FLOT1-ALK binding drives malignant phenotypes of neuroblastoma by activating ALK signaling. *Cancer Res; 74(14); 3790–801. ©2014 AACR.*

Introduction

Anaplastic lymphoma kinase (ALK) is a receptor tyrosine kinase (RTK) that is rather specifically expressed in the nervous system during development in mice (1). ALK was first identified in anaplastic large cell lymphoma as the fusion protein NPM-ALK caused by chromosomal translocation (2). Recently, ALK was highlighted as a therapeutic target of several cancers such as non–small cell lung cancers and colon cancers, which possess oncogenic fusion ALK proteins such as EML4-ALK (3–6). Genetic alterations of ALK have also been identified in cell lines and clinical samples of neuroblastoma, which consist of gene amplifications, activating mutations, or N-terminus truncations (7–12). Activated ALK proteins in neuroblastoma are distinct from other tumors as for the point that they retain the transmembrane domain. The survival of neuroblastoma cells with activated ALK is dependent on the ALK protein in some cases, which highlights the so called oncogene addiction to activated ALK (13).

Neuroblastoma is one of the most refractory solid tumors in children with 5-year survival rates of less than 40% following conventional treatments (14–16). To this end, clinical trials involving patients with neuroblastoma and ALK inhibitors such as crizotinib have already begun (17). However, it was reported that neuroblastoma harboring certain types of activation mutations of ALK show greater resistance to the ALK inhibitors (18) and that there are differences in the malignancy grades among neuroblastoma cases with mutant ALK depending on the type of mutations (19, 20). Therefore, further investigation is necessary to elucidate what aspects of the mutant ALK protein determine the clinicopathological features of neuroblastoma.

As ALK is a RTK, it is essential to understand the signal transduction pathways that mediate the activation of this kinase. In addition to the common downstream mediators of RTKs, such as Akt, Erk, and STAT3, we have shown the critical role of ShcC as a binding partner of ALK in neuroblastoma (21, 22). Further identification of the tyrosine-phosphorylated binding partners of ALK and analysis of their functions in neuroblastoma will aid understanding of the unique oncogenic roles of ALK signaling.

Flotillin-1 (FLOT1) is a plasma membrane lipid raft-localizing protein that is involved in internalization of membrane-localizing proteins into the cytosol by endocytosis. In addition, FLOT1 plays a role in the regulation of actin organization and neuronal regeneration (23, 24), and phosphorylation of FLOT1

Authors' Affiliations: [1]Division of Metastasis and Invasion Signaling, National Cancer Center Research Institute; [2]Department of Cell Therapy and Transplantation Medicine, Graduate School of medicine, The University of Tokyo, Tokyo; [3]Department of Neurosurgery, National Defense Medical College, Saitama; [4]Department of Applied Chemistry, National Defense Academy, Kanagawa; [5]Department of Molecular Pharmacology, National Cerebral and Cardiovascular Center Research Institute, Osaka; [6]Divisions of Cancer Genomics and [7]Biochemistry and Innovative Cancer, Chiba Cancer Center Research Institute, Chiba; and [8]Department of Molecular Cancer Science, Yamagata University School of Medicine, Yamagata, Japan

Note: Supplementary data for this article are available at Cancer Research Online (http://cancerres.aacrjournals.org/).

Corresponding Author: Ryuichi Sakai, Division of Metastasis and Invasion Signaling, National Cancer Center Research Institute, 5-1-1, Tsukiji, Chuo-ku, Tokyo 104-0045, Japan. Phone: 81-3-3542-2511; Fax: 81-3-3542-8170; E-mail: rsakai@ncc.go.jp

doi: 10.1158/0008-5472.CAN-14-0241

Published OnlineFirst May 15, 2014; DOI: 10.1158/0008-5472.CAN-14-0241

at the tyrosine or serine is necessary during internalization (25, 26). At present, there is only limited information about the involvement of FLOT1 in the oncogenicity of solid cancers other than neuroblastoma (27–29). In this report, we identified FLOT1 during the screening of ALK-binding tyrosine-phosphorylated proteins in neuroblastoma cells by using mass spectrometry analysis. Functional analysis revealed that FLOT1 controls the malignant properties of neuroblastoma by regulating the endocytosis and degradation of membrane-localizing ALK protein. It was also suggested that alterations to the binding affinity to FLOT1 in some of the ALK mutants might contribute to the enhancement of oncogenic ALK signaling in neuroblastoma.

Materials and Methods

Antibodies and plasmids

The rabbit ALK antibody was previously described (22). The antibodies against phospho-ALK, Akt, phospho-Akt, p44/42 MAPK (ERK1/2), phospho-ERK1/2, STAT3, phospho-STAT3, and p53 were purchased from Cell Signaling Technology. Other antibodies used are: ALK (H260), clathrin HC, and LAMP2 (Santa Cruz Biotechnology); FLOT1, N-cadherin, and caveolin-1 (BD Transduction Laboratories); FLAG M2 and α-tubulin (Sigma); HA (Nakarai Tesque); and phosphotyrosine (4G10; Upstate Biotechnology).

The cDNAs of human wild-type (WT) *ALK*, the activating mutants of *ALK* (F1174L, K1062M, and R1275Q) and WT *FLOT1* were subcloned into the pcDNA3.1 vector.

Cell culture and tissue samples

NB-39-nu and Nagai human neuroblastoma cell lines were provided by Carcinogenesis Division, National Cancer Center Research Institute (Tokyo, Japan) in 2001 (30). TNB-1 human neuroblastoma cell line was obtained from Human Science Research Resource Bank in 2001 (31). Gene amplification of *MYCN* in these three lines and of *ALK* in NB-39-nu and Nagai is periodically checked to confirm the neuroblastoma origin of these cell lines, most recently in March 2014 (22). The cells were maintained in RPMI-1640 medium (Invitrogen) supplemented with 10% FBS, 10 U/mL penicillin, and 10 μg/mL streptomycin at 37°C in a humidified atmosphere containing 5% CO_2. Human neuroblastoma tissue samples were prepared as previously described (32).

Transfection and establishment of stable clones

Of note, 20 nmol/L of Stealth Select RNAi (Invitrogen) or 4 μg of plasmid was transfected by electroporation using the NEON system (Invitrogen). The siRNA sequences are described in Supplementary Materials and Methods. For establishment of stable ALK-mutant clones, TNB-1 cells were continuously treated with 400 μg/mL of G418. TNB-1 cells stably expressing control or *FLOT1* shRNA were established using lentiviral particles according to the manufacturer's instructions (Santa Cruz Biotechnology).

Purification of ALK-binding tyrosine-phosphorylated proteins

The immunoafffinity purification methods previously described (33) were modified and used for isolation of the ALK-binding tyrosine-phosphorylated proteins. The detailed protocol is described in Supplementary Materials and Methods.

Immunoblotting, immunoprecipitation, and immunofluorescence

The immunoblotting, immunoprecipitation, and immunofluorescence were done as described previously (26, 32) with modifications. The detailed protocols are described in Supplementary Materials and Methods.

Pulse-chase analysis of ALK internalization

Cells cultured on coverslips were incubated with cold complete medium for 5 minutes at 4°C and then with medium containing 4 μg/mL of anti-ALK (H260) antibody for 30 minutes at 4°C. After removing the medium, the cells were cultured in fresh medium at 37°C for the indicated time period. The cells were fixed and stained with the fluorescence-conjugated secondary antibody. For colocalization analysis, the cells were also stained for FLOT1, clathrin, or caveolin-1. The cells have cytosolic colocalization signals (diameter > 2 μm) and were counted using fluorescence images and ImageJ software. At least 200 cells per sample were counted, and the percentage of positive cells was calculated.

Biotinylation and purification of plasma membrane–localized proteins

A total of 5×10^7 cells were incubated with cold complete medium for 5 minutes at 4°C. The cell surface proteins were labeled with 200 μg sulfo-NHSS-biotin (Thermo Scientific) for 40 minutes at 4°C. After cell lysis, biotinylated proteins were immunoprecipitated using Ultralink Immobilized NeutrAvidin protein (Thermo Scientific). For internalization assay, the labeled cells were cultured in fresh complete medium at 37°C for 60 minutes. The cell surface biotin was stripped by incubation with 180 mmol/L sodium 2-mercaptoethane sulfonate (MesNa; Sigma). After quenching the MesNa by the addition of 180 mmol/L iodoacetamide (Sigma) for 10 minutes, the biotinylated proteins were immunoprecipitated.

Cell migration assay

The cells (1×10^4) were seeded onto the upper part of the Transwell inserts (BD Falcon) coated with fibronectin. The migrated cells on the lower surface of the filter were fixed and stained with Giemsa's stain solution. The number of migrated cells was counted using a BX51 microscope (Olympus).

Cell death assay

The cellular nuclei stained with 100 μmol/L Hoechst 33342 and 4.0 μg/mL propidium iodide (PI; Thermo Scientific) were independently counted using a fluorescence microscope (IX81-ZDC-DSU; Olympus). At least 500 cells per sample were examined and the percentage of PI-positive cells to total Hoechst-positive cells was calculated.

Anchorage-independent cell proliferation assay

Cells were cultured on MPC-coated plates (Thermo Scientific) at 1×10^3 cells per 6 wells for 7 days and the total numbers of cells were counted.

Published OnlineFirst May 15, 2014; DOI: 10.1158/0008-5472.CAN-14-0241

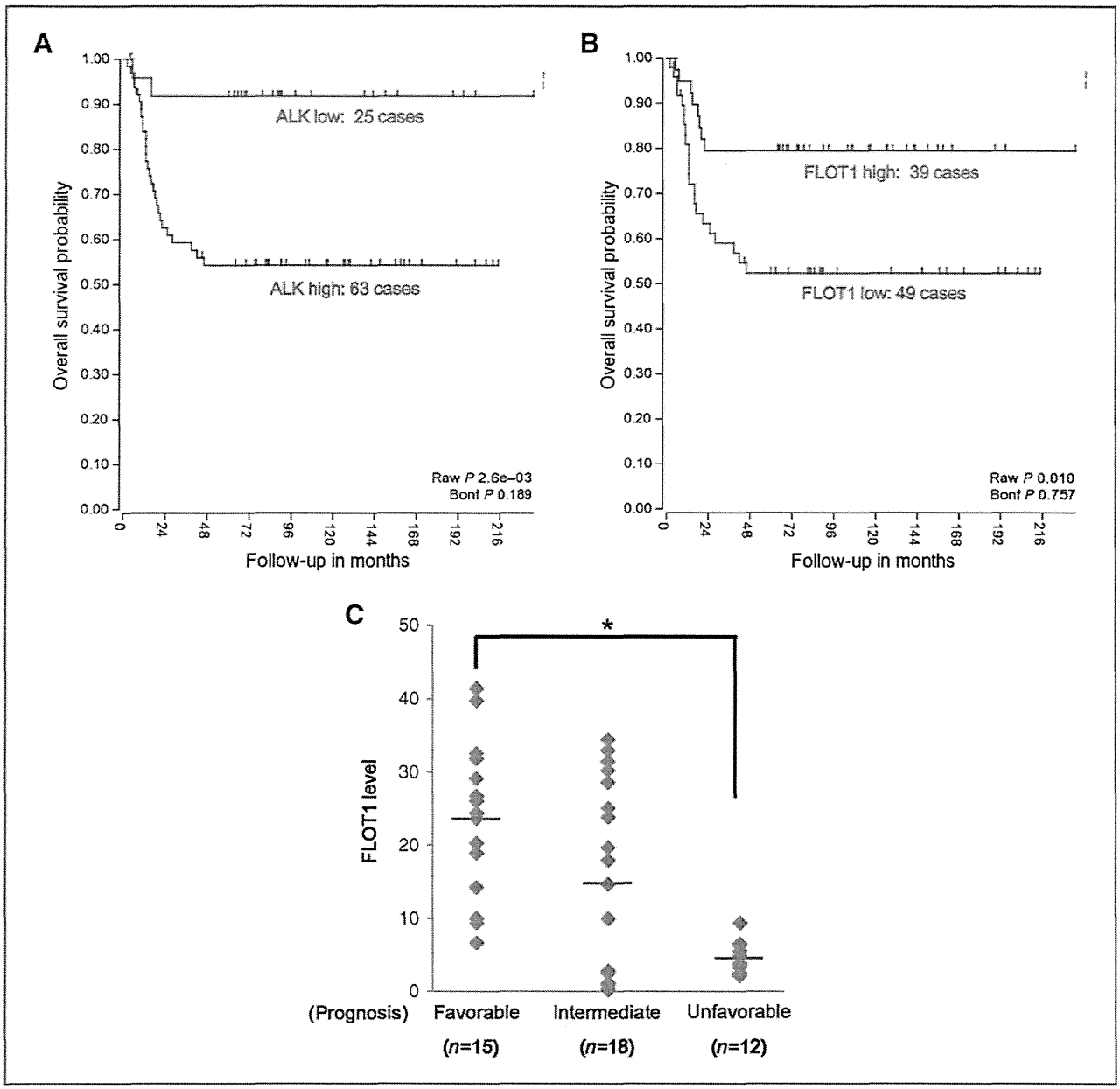

Figure 1. Clinical impact of FLOT1 expression in neuroblastoma cases. A and B, Kaplan–Meier analysis of overall survival in patients with neuroblastoma with the classifications based on *ALK* (A) and *FLOT1* (B) mRNA expression. The data were obtained from the R2 microarray public database (http://r2.amc.nl). C, ten protein samples from clinical neuroblastoma specimens classified by Brodeur's classification (favorable, 15 cases; intermediate, 18 cases; unfavorable, 12 cases) were subjected to immunoblotting using the FLOT1 antibody and the expression levels of FLOT1 were quantified. Red bars, average values. *, $P < 0.01$.

Tumor xenograft assay

The animal experimental protocols were approved by the Committee for Ethics of Animal Experimentation, and the experiments were conducted in accordance with the guidelines for animal experiments in the National Cancer Center. TNB-1 cells (5×10^6) were subcutaneously injected into the bilateral flank of female 6-week-old BALB/c nude mice (Clea Japan). At 6 weeks after tumor inoculation, the mice were sacrificed, and the subcutaneous tumors were excised with the attached muscle layers. The tumor volume was calculated with the equation (length $\times$ width^2)/2 and the tumor weight (g) was measured. The tumor tissue was stained by hematoxylin and eosin (H&E).

Statistical analysis

The data for all the quantitative results are expressed as mean and SD from three independent experiments. Plotting of scatter graphs and testing of difference of means by

Published OnlineFirst May 15, 2014; DOI: 10.1158/0008-5472.CAN-14-0241

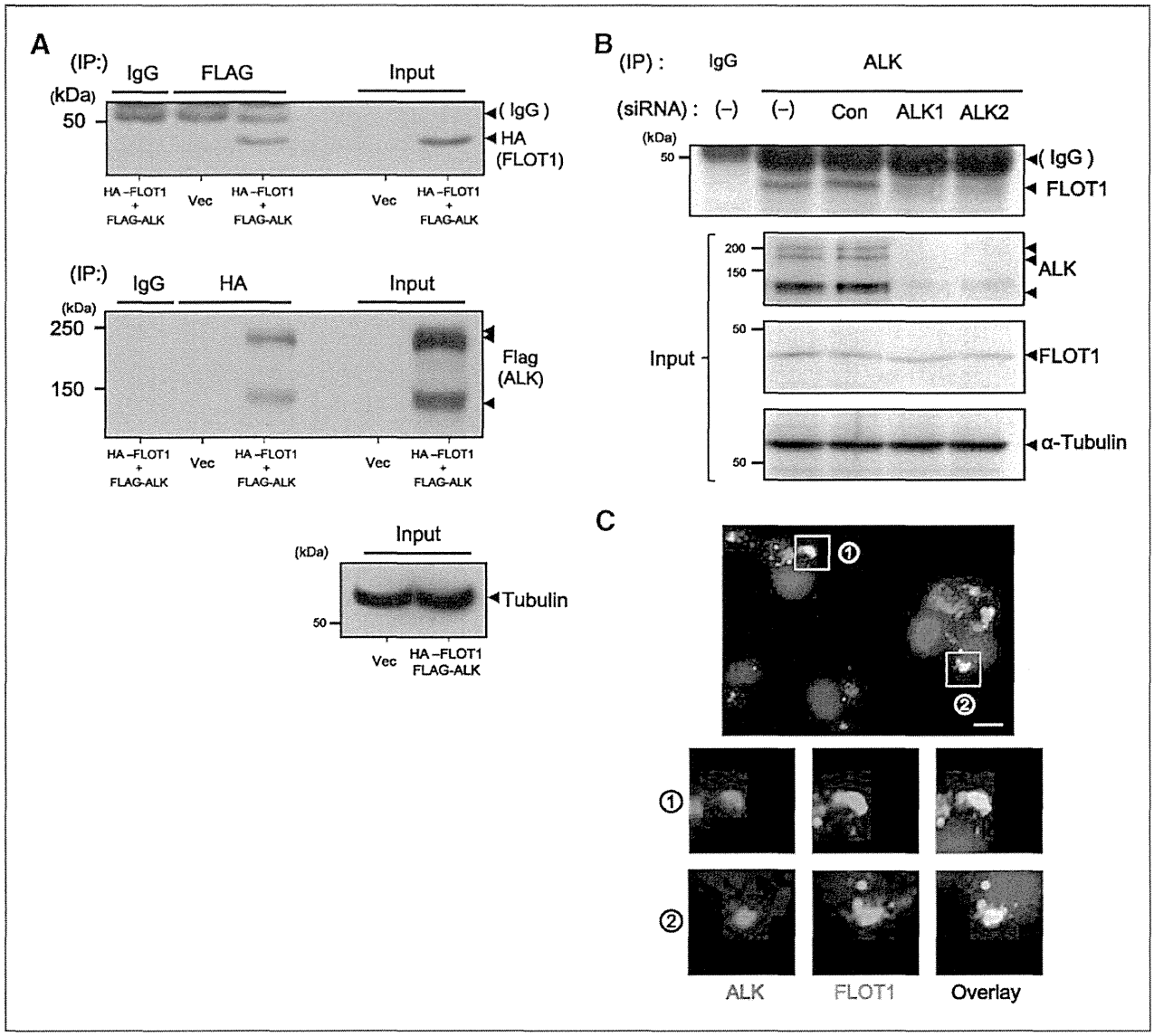

Figure 2. FLOT1 interacts with ALK in neuroblastoma cells. A, Cos-7 cells were transiently transfected with an empty vector (vector), flag-tagged WT *ALK*, or HA-tagged WT *FLOT1* for 12 hours. The cell lysates were immunoprecipitated with control IgG, anti-FLAG antibody (ALK), or anti-HA antibody (FLOT1) and the immunocomplexes and total cell lysates (input) were analyzed by immunoblotting using the indicated antibodies. B, NB-39-nu neuroblastoma cells were transiently transfected with control siRNA (Con) or one of the two siRNAs against *ALK* (ALK1 and ALK2) for 72 hours. The cell lysates were immunoprecipitated with the indicated antibodies and subjected to immunoblotting. C, NB-39-nu cells were stained with DAPI (blue) and antibodies against ALK (red) and FLOT1 (green), and were observed by confocal microscopy. The submembrane regions of the dorsal cell membrane were imaged. Bottom panels are magnified images of the boxed regions. Arrows, colocalization of ALK and FLOT1. Bar, 10 μm.

Student *t* test were achieved using Microsoft Excel 2007 software. *P* values of <0.01 were considered as statistically significant.

Results

Identification of FLOT1 as a binding partner and kinase substrate of ALK in neuroblastoma

To identify the phosphotyrosine-containing proteins associated with ALK, we performed two-step affinity purification using TNB-1 neuroblastoma cells, which stably expresses the ALK protein tagged with FLAG at the C-terminus as described in Supplementary Fig. S1. Mass spectrometry analysis identified several reported binding partners of ALK such as ShcA, ShcC, and IRS1 (22, 34) along with numbers of novel candidates of ALK-binding phosphoproteins. Association of these novel candidates with ALK was confirmed by immunoprecipitation analysis using available antibodies and further association with prognosis of neuroblastoma was checked using public database to estimate clinical impact. In this study, we focused on FLOT1 among these ALK-binding proteins through these screening.

Published OnlineFirst May 15, 2014; DOI: 10.1158/0008-5472.CAN-14-0241

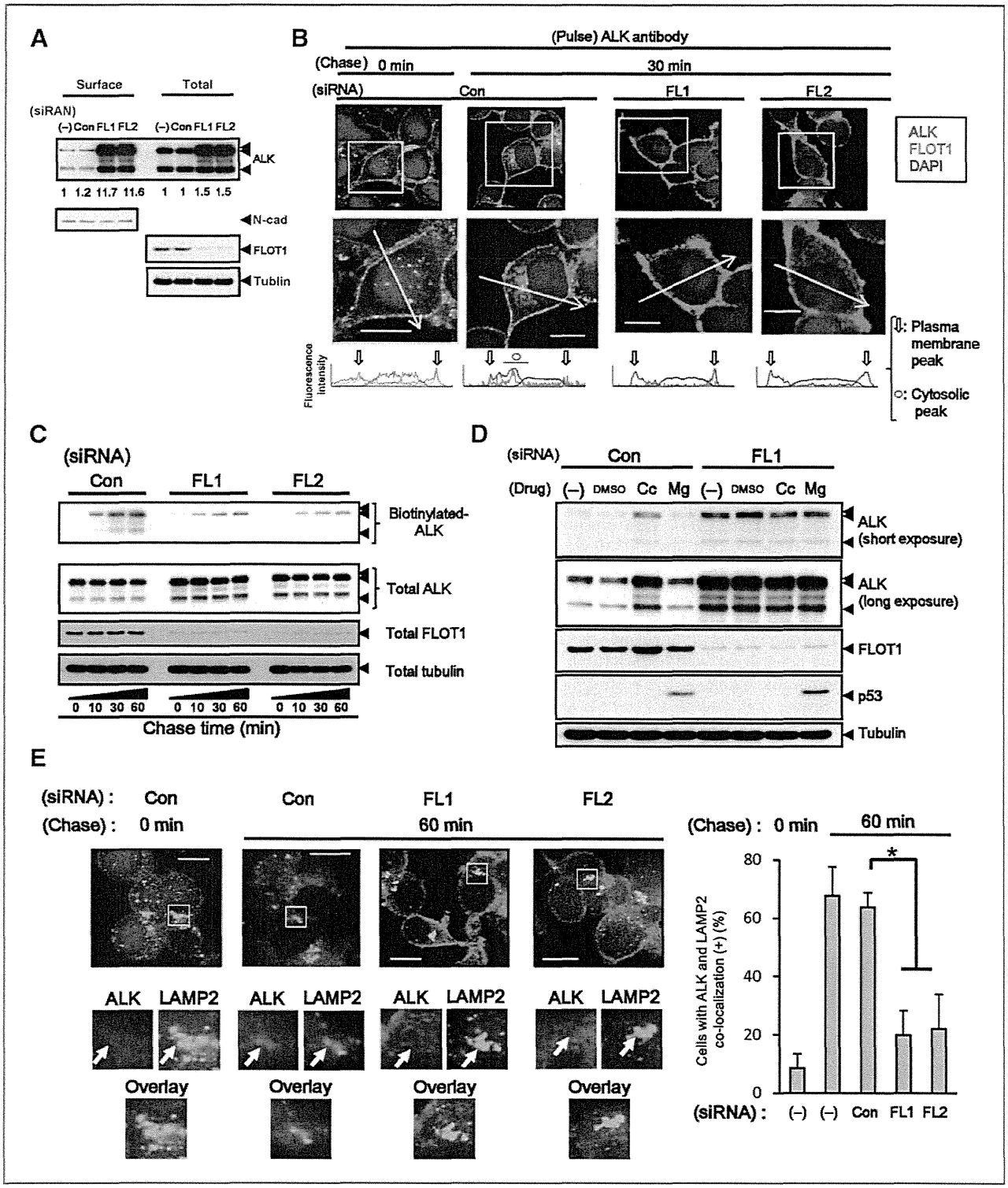

Figure 3. FLOT1 regulates endocytosis and cell surface expression of ALK. A, NB-39-nu cells were treated with control siRNA (con) or *FLOT1* siRNA (FL1 and FL2) for 72 hours. The plasma membrane–localized proteins were purified as described in Materials and Methods and analyzed by immunoblotting using the ALK antibody or N-cadherin antibody. Total cell lysates were also analyzed by immunoblotting using the indicated antibodies. The levels of ALK in each sample were quantified and denoted as relative value [siRNA (–) = 1] under immunoblotting data. B, NB-39-nu cells treated with indicated siRNAs were subjected to pulse-chase analyses by using an ALK antibody (red). The cells were stained with DAPI (blue) and FLOT1 antibody (green) and observed by confocal microscopy. The lower images are magnified images of the boxed regions. Fluorescent intensity of each signal was quantified by line scan analysis as indicated by yellow arrows and depicted as histograms. (*Continued on the following page.*)

Published OnlineFirst May 15, 2014; DOI: 10.1158/0008-5472.CAN-14-0241

The R2 database, one of the largest public databases of microarray in neuroblastoma cases (http://r2.amc.nl), indicated that high expression levels of ALK mRNA significantly correlates with poor prognosis in patients with neuroblastoma (Fig. 1A), suggesting that ALK signaling has clinical impact even in patients without genetic alteration of ALK. On the other hand, low expression of FLOT1 mRNA was positively correlated with poor prognosis of clinical neuroblastoma cases in the R2 database (Fig. 1B). We also analyzed the expression of FLOT1 and ALK proteins in specimens from 45 clinical neuroblastoma cases, which belong to three clinical malignancy grades (favorable, 15 cases; intermediate, 18 cases; unfavorable, 12 cases) as classified by Brodeur's classification (35, 36), and demonstrated that the levels of FLOT1 expression inversely correlate with clinical malignancy grade (Fig. 1C). A representative blot of five samples from each group is shown in Supplementary Fig. S2.

Because FLOT1 expression has apparent association with prognosis and clinical grades of neuroblastoma, we hypothesized that FLOT1 regulates oncogenic potentials of neuroblastoma through association of ALK. The binding of ALK to FLOT1 was confirmed by immunoprecipitation analysis using anti-FLAG or anti-HA antibodies in COS-7 cells expressing FLAG-tagged ALK and HA-tagged FLOT1 (Fig. 2A). Binding of ALK to endogenous FLOT1, as well as ALK-mediated tyrosine-phosphorylation of FLOT1, was also demonstrated in NB-39-nu neuroblastoma cells harboring amplified ALK (Fig. 2B and Supplementary Fig. S3). By immunocytostaining analysis, ALK and FLOT1 were mainly colocalized within the cytoplasm, especially at the submembrane regions of the ventral membrane (Fig. 2C). These results suggested that FLOT1 is associated with ALK as a binding partner and kinase substrate in neuroblastoma cells.

FLOT1 regulates degradation of ALK in lysosome through endocytosis

Considering that FLOT1 is reported to be involved in endocytosis of membrane proteins, we investigated the effect of FLOT1 knockdown on the amount of membrane-localizing ALK. The amount of ALK protein at the plasma membrane was markedly increased by treatment with either of two FLOT1 siRNAs, which resulted in rather moderate increases in total ALK protein levels (Fig. 3A). Pulse-chase analysis with an ALK antibody revealed marked reduction in the amount of internalized ALK in the NB-39-nu cells treated with each FLOT1 siRNA at the time point of 30 minutes (Fig. 3B). Biotinylation internalization analysis confirmed that gradual increase in the total amount of internalized ALK was significantly impaired by treatment with each FLOT1 siRNA (Fig. 3C). These results suggested that FLOT1 regulates the amount of ALK on the cell surface through endocytosis.

Membrane proteins that are internalized by endocytosis are usually degraded by the proteasome or lysosome (37). Degradation of ALK was inhibited following treatment with the lysosomal inhibitor concanamycin, while it was not significantly affected by the proteasomal inhibitor MG132 (Fig. 3D). Under the presence of concanamycin, accumulation of ALK at plasma membrane was observed by knockdown of FLOT1, whereas total ALK protein level was less affected (Supplementary Fig. S4A). Pulse-chase analysis visualized by immunocytostaining demonstrated the colocalization of internalized ALK with the lysosomal marker LAMP2 that was disrupted by treatment with FLOT1 siRNA (Fig. 3E). Colocalization of FLOT1 with internalized ALK was also observed at the early phase of endocytosis, whereas no obvious colocalization of ALK with the other known endosomal transporters, clathrin heavy chain and caveolin-1 (38, 39), was observed (Supplementary Fig. S4B and S4C). These results indicated that FLOT1 regulates lysosomal degradation of ALK through clathrin/caveolin-independent endocytosis.

FLOT1 regulates ALK signaling through modulation of the amount of cell-surface ALK

Phosphorylation of ALK as well as known downstream mediators of ALK such as AKT, ERK1/2, and STAT3, was increased in the NB-39-nu cells treated with FLOT1 siRNA (Fig. 4A). The increased levels of phosphorylation of these molecules were all subsequently reduced by treatment with either ALK siRNA or NVP-TAE-684, an inhibitor of ALK. We further analyzed whether the expression of FLOT1 affects the oncogenic properties of activated ALK in NB-39-nu neuroblastoma (13, 22). Induction of anchorage-independent growth, resistance to the anticancer agent *cis*-diamminedichloroplatinum (cisplatin; CDDP), and cell migration were enhanced by the treatment of NB-39-nu cells with FLOT1 siRNA (Fig. 4B and Supplementary Fig. S5A and S5B). Similar results were also obtained using Nagai, another neuroblastoma cell line harboring amplified WT ALK (Supplementary Fig. S6A and S6B). On the other hand, reduced expression and phosphorylation of ALK, and phosphorylation of AKT, ERK1/2, and STAT3 as well as induction of cell death, decreased proliferation, and acceleration of ALK internalization were observed by overexpression of FLOT1 in NB-39-nu cells (Fig. 4C and D and Supplementary Fig. S5C and S5D).

To investigate whether FLOT1 has the same regulatory roles of ALK in neuroblastoma cells harboring single-copy ALK, TNB-1 cell lines stably expresses FLOT1 shRNA, TNB-FL1 and TNB-FL2 were established (Fig. 4E). Two control

(*Continued.*) Open arrows and circles indicate peaks of the fluorescence signals for the plasma membrane and the cytosol, respectively. Bar, 10 μm. C, the siRNA-treated NB-39-nu cells were subjected to ALK-internalization assays at the indicated time points as described in Materials and Methods. The avidin-bounded (internalized) proteins and total cell lysates were analyzed by immunoblotting using the indicated antibodies. D, NB-39-nu cells treated with siRNAs were cultured in the presence of DMSO, lysosomal inhibitor concanamycin (Cc, 10 μmol/L), or proteasomal inhibitor MG132 (MG, 15 μmol/L) for 8 hours and subjected to immunoblotting. p53 was analyzed as a representative protein degraded by proteasome. E, NB-39-nu cells were treated with siRNAs and pulse-chased with an ALK antibody (red). The cells were stained with DAPI (blue) and LAMP2 antibody (green). Bottom panels are magnified images of the boxed regions. Cells with ALK positive and LAMP2-positive dots were quantified as described in Materials and Methods (right bar graph). Bar, 10 μm. *, $P < 0.01$.

Published OnlineFirst May 15, 2014; DOI: 10.1158/0008-5472.CAN-14-0241

lines of TNB-1 cells, TNB-Con1 and TNB-Con2 cells, were also established using the control vector. Enhanced expression of ALK and phosphorylation of AKT and ERK1/2 was observed in TNB-FL1 and TNB-FL2 cells, whereas no significant changes in the expression of other RTKs, such as EGFR, RET, and TrkB, were observed (Fig. 4E). In addition, increased anchorage-independent growth was detected in the TNB-FL1 and TNB-FL2 cells, which was blocked by treatment with the ALK inhibitor (Fig. 4F and Supplementary Fig. S5E). These results demonstrated that FLOT1 inhibits the malignant phenotype of neuroblastoma cells through endocytosis of ALK.

Activating mutations of ALK have low binding affinities to FLOT-1 and cause ALK stabilization and malignant phenotypes in neuroblastoma cells

It is reported that some of the activating mutations of ALK such as the common F1174L mutation exhibit more malignant phenotypes and poor prognosis than others (19), while the mechanisms causing the differences are still not clear. We investigated differences in the binding affinities between mutant ALK proteins and FLOT1 by using TNB-1 neuroblastoma cells stably expressing WT, F1174L (FL; mutation near the c-helix loop), K1268M (KM; mutation in the juxtamembrane domain), and R1275Q (RQ; mutation near the ATP-binding domain) mutants of ALK (8–11). FLOT1 steadily associated with the WT and RQ mutants of ALK, but not as efficiently with the FL and KM mutants (Fig. 5A). Furthermore, knockdown of FLOT1 affected the internalization of biotinylated ALK in the WT and RQ mutants but not in the FL and KM mutants (Fig. 5B). In addition, the phosphorylation levels of ALK, AKT, and ERK1/2 were not obviously elevated by treatment with FLOT1 siRNA in the TNB-1 cells with the FL or KM mutation (Fig. 5B).

Anchorage-independent growth was significantly enhanced by FLOT1 siRNA in cells expressing WT or RQ mutant, whereas no obvious changes were observed in the cells expressing the FL and KM mutants, which originally showed enhanced anchorage-independent growth. Anchorage-independent growth of all the cells analyzed was reduced by treatment with the ALK inhibitor (Fig. 5C). Similar difference in ALK mutants were also confirmed using the TNB-1 cells expressing WT ALK, the FL mutant, and the KM mutant as for resistance to CDDP and cell migration (Supplementary Fig. S7A and S7B). These results suggested that some of the activating mutations of ALK might have enhanced stability at the cell membrane by reduced affinity to FLOT1, which leads to further enhancement of the malignancy of neuroblastoma.

FLOT1 regulates tumorigenicity of neuroblastoma cells

To investigate the role of FLOT1 in the tumorigenicity of neuroblastoma, TNB-Con1/2, and TNB-FL1/2 cells were subcutaneously injected into nude mice (Fig. 6A). Because of the low tumorigenicity of the original TNB-1 cells, tumors were not detectably formed at 6 weeks following injection of TNB-Con cells. On the other hand, tumors as large as 10 to 40 mm in diameter were clearly formed by the TNB-FL1 and TNB-FL2 cells in this period (Fig. 6A). Histologic study of these tumors revealed that the tumor cells had infiltrated into the muscle layers and formed large intratumoral vessels, which reflects the malignant phenotype of the tumors (Fig. 6B). These results indicated that FLOT1 might be a negative regulator of the malignant characteristics of neuroblastoma *in vivo*. Along with the results indicating that the low expression of FLOT1 is significantly associated with poor prognosis and unfavorable histologic grades of neuroblastoma (Fig. 1B and C), it was indicated that deregulation of FLOT1 expression is involved in the progression of neuroblastoma through enhancement of ALK signaling.

Discussion

Deregulation of the RTK ALK by amplification or activating mutation of the *ALK* gene has been reported in 10% to 15% of human neuroblastoma cases, in which the relationship between ALK signaling and oncogenesis of neuroblastoma is indicated. Although the association between ALK expression and poor prognosis of neuroblastoma is observed (Fig. 1A), it is not clear whether different modes of activation of ALK signaling are involved in the progression of the other neuroblastoma cases. In this study, we provided *in vitro* and *in vivo* evidence that activation of ALK signaling caused by impaired FLOT1-mediated endocytosis is associated with malignancy of neuroblastoma cells. This finding was supported by the observation that FLOT1 expression levels in the clinical samples is inversely correlated with prognosis of the disease in a public database (Fig. 1B) and grades of malignancy in tissue samples (Fig. 1C). Taken together, the novel tumor-suppressing role of FLOT1 in the majority of neuroblastoma that lacks genetic alterations of *ALK* was implied.

There was tendency that the low expression level of FLOT1 is associated with high expression levels of ALK in the neuroblastoma tissues used for Fig. 1C, while it was not statistically significant possibly due to limited numbers of tissues examined (data not shown). Therefore, we could not completely exclude the possibility that FLOT1 also degrades signaling molecules other than ALK, which are associated with malignancy of neuroblastoma, although it was confirmed that FLOT1 preferably regulates the ALK protein among several other RTKs expressed in neuroblastoma (Fig. 4E). The information about the involvement of FLOT1 in cancer development is still limited (29, 40–42). It was recently suggested that FLOT1 is associated with poor prognosis of breast cancer as a result of stabilization of ErbB2 (27) and also plays oncogenic roles in esophageal cancer and hepatocellular carcinoma (28, 40). It is speculated that FLOT1 might regulate the organ-dependent target proteins and functions in the development of cancers and the regulation is rather selective to ALK in neuroblastoma. Considering that activated ALK found in other types of cancers lack transmembrane domain, the accumulation of membranous ALK by deficient FLOT1 might be etiological only in neuroblastoma.

It has been reported that FLOT1 physiologically acts as an endosomal transporter of membrane proteins (23–25). Further study is required to clarify the precise mechanisms